22 ATMOSPHERIC OPTICS

Contents

Light can be considered as photon particles or electromagnetic waves, either of which travel along paths called **rays**. To first order, light rays are straight lines within a uniform transparent medium such as air or water, but can **reflect** (bounce back) or **refract** (bend) at an interface between two media. Gradual refraction (curved ray paths) can also occur within a single medium containing a smooth variation of optical properties.

The beauty of nature and the utility of physics come together in the explanation of rainbows, halos, and myriad other atmospheric optical phenomena.

22.1. RAY GEOMETRY

When a **monochromatic** (single color) light ray reaches an interface between two media such as air and water, a portion of the incident light from the air can be reflected back into the air, some can be refracted as it enters the water (Fig. 22.1), and some can be absorbed and changed into heat (not sketched). Similar processes occur across an air-ice interface.

22.1.1. Reflection

The angle θ_3 of the reflected ray always equals the angle θ_1 of the incident ray, measured with respect to a line normal (perpendicular) to the interface:

$$\theta_1 = \theta_3 \qquad \bullet(22.1)$$

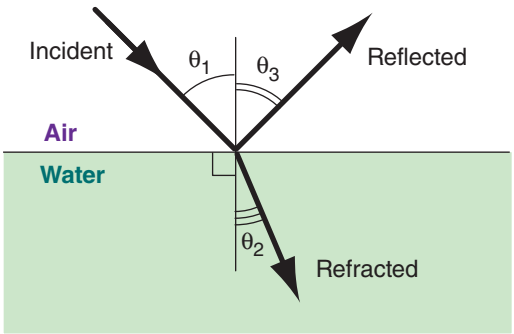

Figure 22.1
Geometric optics at an air-water interface. Black arrows are light-ray paths.

Sample Application

Rays of red and violet light in air strike a water surface, both with incident angle of 60°. Find the angle of refraction for each color, given T = 20°C, P = 101 kPa?

Find the Answer

Given: $\theta_1 = 60°$, $T = 20°C$, $P = 101$ kPa
Find: $\theta_2 = ?°$ for red (λ=0.7 μm) and violet (λ=0.4 μm).

Use eq. (22.5):
$\theta_2 = \arcsin[(n_1/n_2)\cdot\sin(\theta_1)] = \arcsin[\mu_{12}\cdot\sin(\theta_1)]$
with μ_{12} from eq. (22.3) and refractive indices from Table 22-1.

For red: $\mu_{12} = n_1/n_2 = 1.0002704/1.3305 = 0.7518$
$\theta_2 = \arcsin[0.7518\cdot\sin(60°)]$
$\theta_2 = \underline{\mathbf{40.62°}}$
Similarly for violet: $\theta_2 = \underline{\mathbf{40.15°}}$

Check: Units OK. Physics OK.
Exposition: Had there been no bending, then both answers would have been 60°. Angles closer to 60° for this example correspond to less bending. The answers above confirm the statement that red light is bent less than violet. The **amount of bending** (difference between incident and refracted angles) is large: 60° – 40° = 20°.

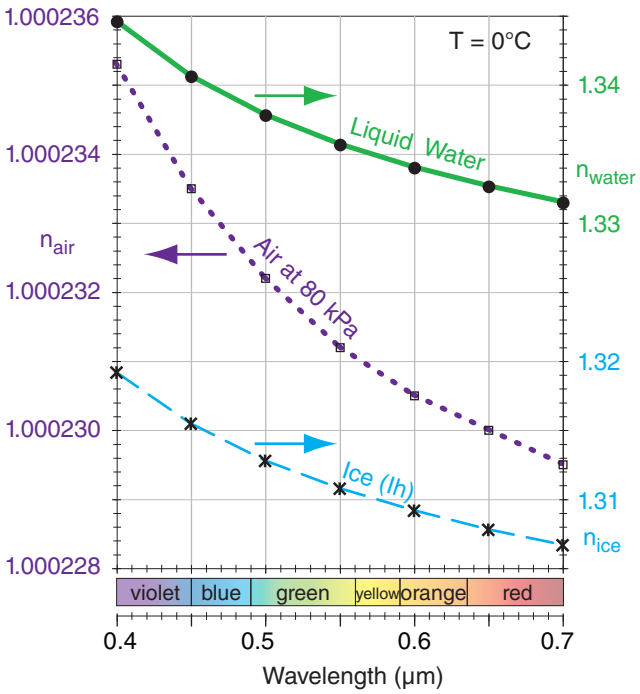

Figure 22.2
Refractive index n for various wavelengths of visible light at T = 0°C. See Table 22-1 for details. The wavelength bands that we perceive as different **colors** *is approximate, and is slightly different for each person. In this chapter we will use red ≈ 0.7 μm, orange ≈ 0.62 μm, yellow ≈ 0.58 μm, green ≈ 0.53 μm, blue ≈ 0.47 μm, and violet ≈ 0.4 μm wavelength.*

The reflected angle does not depend on color (i.e., is not a function of the wavelength of light).

22.1.2. Refraction

22.1.2.1. Refractive index

The **refractive index** n_i for medium i relative to a vacuum is defined as:

$$n_i = \frac{c_o}{c_i} \qquad \bullet(22.2)$$

where c_i is the speed of light through medium i and $c_o = 3 \times 10^8$ m s^{-1} is the speed of light in a vacuum.

The ratio of refractive indices is sometimes defined as:

$$\mu_{12} = \frac{n_1}{n_2} \qquad \bullet(22.3)$$

where subscripts 1 and 2 refer to the media containing the incident ray and refracted rays, respectively. Different colors and different media have different refractive indices, as indicated in Table 22-1 and Fig. 22.2.

22.1.2.2. Snell's Law

The relationship between the incident angle θ_1 and refracted angle θ_2 (Fig. 22.1) is called **Snell's Law**:

$$\frac{\sin\theta_1}{\sin\theta_2} = \frac{c_1}{c_2} = \frac{n_2}{n_1} = \frac{1}{\mu_{12}} \qquad \bullet(22.4)$$

Incident and refracted rays are always in the same plane. This plane includes the line that is normal to the surface. It is the plane that gives the smallest angle between the incident ray and the surface.

Solving Snell's Law for the refracted ray angle gives:

$$\theta_2 = \arcsin[\mu_{12}\cdot\sin(\theta_1)] \qquad (22.5)$$

Red light is bent less than violet light as it passes through an interface. Thus, refraction causes white light to be spread into a **spectrum** of colors. This phenomenon is called **dispersion**.

A viewer looking <u>toward</u> the incoming light ray (Fig. 22.3) would see a **light point** in the celestial sphere overhead at angle θ_2 from normal.

22.1.2.3. Snell's Law in 3 Dimensions

Sometimes it is easier to work with x and y components of the incident ray, where the x-axis might be aligned with the axis of a columnar ice crystal, for example, and the y-axis might be on the crystal prism surface (Fig. 22.3). The relationship between the component angles and the incident angle is:

Table 22-1a. Refractive index (n_{air}) for **air** with pressure P = 101.325 kPa and relative humidity RH = 75%. *From NIST.*

λ (μm)	Temperature (°C)				
	–40	**–20**	**0**	**20**	**40**
0.4 violet	1.0003496	1.0003219	1.0002982	1.0002773	1.0002583
0.45	1.0003469	1.0003194	1.0002958	1.0002751	1.0002562
0.5	1.0003450	1.0003176	1.0002942	1.0002736	1.0002548
0.55	1.0003436	1.0003163	1.0002930	1.0002725	1.0002537
0.6	1.0003425	1.0003154	1.0002921	1.0002716	1.0002529
0.65	1.0003417	1.0003146	1.0002914	1.0002710	1.0002523
0.7 red	1.0003410	1.0003140	1.0002908	1.0002704	1.0002518

Table 22-1b. Refractive index (n_{air}) for **air** with P = 80 kPa and RH = 75%. *Based on data from NIST modified Edlen Eq. calculator.*

λ (μm)	Temperature (°C)				
	–40	**–20**	**0**	**20**	**40**
0.4 violet	1.0002760	1.0002541	1.0002353	1.0002188	1.0002036
0.45	1.0002738	1.0002521	1.0002335	1.0002171	1.0002019
0.5	1.0002723	1.0002507	1.0002322	1.0002158	1.0002008
0.55	1.0002712	1.0002497	1.0002312	1.0002150	1.0001999
0.6	1.0002704	1.0002489	1.0002305	1.0002143	1.0001993
0.65	1.0002697	1.0002483	1.0002300	1.0002138	1.0001988
0.7 red	1.0002692	1.0002479	1.0002295	1.0002134	1.0001984

Table 22-1c. Refractive index (n_{air}) for **air** with P = 40 kPa and RH = 75%. *Based on data from NIST modified Edlen Eq. calculator.*

λ (μm)	Temperature (°C)				
	–40	**–20**	**0**	**20**	**40**
0.4 violet	1.0001379	1.0001270	1.0001176	1.0001091	1.0001009
0.45	1.0001369	1.0001260	1.0001166	1.0001082	1.0001000
0.5	1.0001361	1.0001253	1.0001160	1.0001076	1.0000994
0.55	1.0001355	1.0001248	1.0001155	1.0001071	1.0000990
0.6	1.0001351	1.0001244	1.0001151	1.0001068	1.0000987
0.65	1.0001348	1.0001241	1.0001149	1.0001066	1.0000985
0.7 red	1.0001346	1.0001239	1.0001147	1.0001064	1.0000983

Table 22-1d. Refractive index (n_{water}) for **liquid water**. *Based on data from IAPWS 1997 release and CRC Handbook.*

λ (μm)	Temperature (°C)				
	–40	**–20**	**0**	**20**	**40**
0.4 violet	(values below	1.3429	1.3446	1.3436	1.3411
0.45	0°C are for	1.3390	1.3406	1.3396	1.3371
0.5	supercooled	1.3362	1.3378	1.3368	1.3344
0.55	water)	1.3341	1.3357	1.3347	1.3323
0.6		1.3324	1.3340	1.3330	1.3306
0.65		1.3310	1.3326	1.3317	1.3293
0.7 red		1.3299	1.3315	1.3305	1.3281
density (kg m^{-3}):		**993.547**	**999.840**	**998.207**	**992.200**

Table 22-1e. Refractive index (n_{ice}) for **ice (Ih)**. *Based on data from S.G. Warren (1984) and V.F. Petrenko & R.W. Whitworth (1999).*

λ (μm)	Temperature (°C)				
	–40	**–20**	**0**	**20**	**40**
0.4 violet	1.3206	1.3199	1.3192	(values at 0°C were extrapolated)	
0.45	1.3169	1.3162	1.3155		
0.5	1.3142	1.3135	1.3128	(See INFO Box in Precipitation	
0.55	1.3122	1.3115	1.3108	chapter for info on ice phases	
0.6	1.3106	1.3099	1.3092	such as Ih.)	
0.65	1.3092	1.3085	1.3078		
0.7 red	1.3081	1.3074	1.3067		

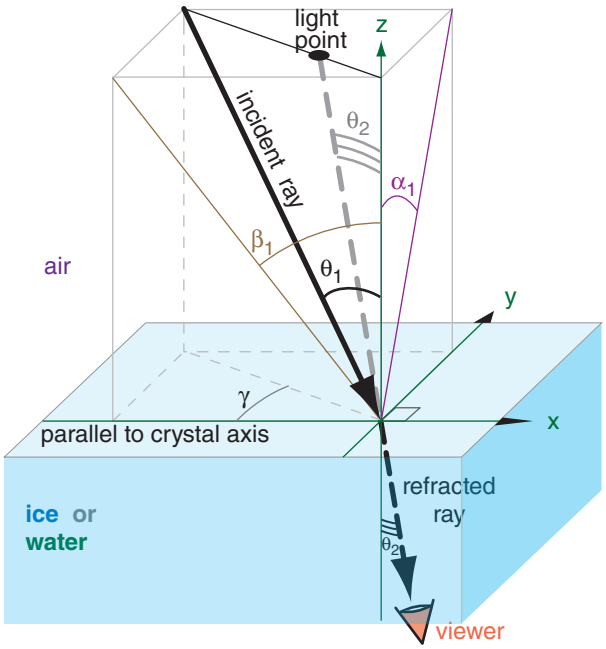

Figure 22.3
Components of refraction geometry. Incident ray is thick black solid arrow. Refracted ray is thick black dashed arrow. The tail (thick grey dashed line) of the refracted ray is extended to show that it lies in the same plane as the incident ray.

Sample Application

A ray of red light in air strikes a water surface, with incidence angle components of $\alpha_1 = 45°$ and $\beta_1 = 54.74°$. What are the corresponding component angles of the refracted ray? Assume $T = 20°C$ and $P = 101.325$ kPa.

Find the Answer

Given: $\alpha_1 = 45°$, $\beta_1 = 54.74°$.
Find: $\alpha_2 = ?°$, $\beta_2 = ?°$

From Table 22-1 for red light:
$\mu_{12}^2 = (1.0002704/1.3305)^2 = (0.7518)^2 = 0.5652$
Also: $\tan(45°) = 1$, and $\tan(54.74°) = 1.414$
Next, solve eq. (22.8):

$$b_{\alpha\beta} = \frac{0.5652}{1+(1-0.5652)\cdot(1+2)} = 0.2453$$

Then use eqs. (22.7):
$\tan^2(\alpha_2) = 0.2453\cdot[\tan^2(45°)] = 0.2453$
$\tan^2(\beta_2) = 0.2453\cdot[\tan^2(54.74°)] = 0.4906$

Thus: $\alpha_2 = \arctan[(0.2453)^{0.5}] = \underline{\mathbf{26.35°}}$
$\beta_2 = \arctan[(0.4906)^{0.5}] = \underline{\mathbf{35.01°}}$

Check: Units OK. Physics OK.
Exposition: Using eq. (22.6) with the incident angle components of 45° and 54.74°, we find that the incident ray angle is $\theta_1 = \arctan[(1+2)^{0.5}] = 60°$. This is the same as a previous Sample Application. Using eq. (22.6) on the answers above, we find $\theta_2 = \arctan[(0.2453+0.4906)^{0.5}] = \underline{\mathbf{40.62°}}$. This is also the same as a previous Sample Application, which verifies eqs. (22.6 - 22.9).

Sample Application

Find the speed of red light through liquid water and through air at $T = 20°C$ and $P = 101.325$ kPa.

Find the Answer

Given: $\lambda = 0.7$ μm, $T = 20°C$ and $P = 101.325$ kPa.
Find: $c_{air} = ?$ m s^{-1} , $c_{water} = ?$ m s^{-1}

Use eq. (22.2) with refractive indices from Table 22-1:
$c_{air} = c_o/n_{air} = (3\text{x}10^8 \text{m s}^{-1})/1.0002704 = \underline{\mathbf{2.999\text{x}10^8}}\ \underline{\mathbf{\text{m s}^{-1}}}$
$c_{water} = c_o/n_{water} = (3\text{x}10^8 \text{m s}^{-1})/1.3305 = \underline{\mathbf{2.255\text{x}10^8}}\ \underline{\mathbf{\text{m s}^{-1}}}$

Check: Speeds reasonable. Units OK.
Exposition: The difference in speeds of light is useful for understanding Huygens' principle.

$$\tan^2\theta_1 = \tan^2\alpha_1 + \tan^2\beta_1 \qquad (22.6)$$

where θ, α and β are as illustrated in Fig. 22.3. This relationship also applies to refracted angles (θ_2, α_2, β_2), and will be used extensively later in this chapter to discuss ice-crystal optics.

Component angles α and β of the refracted and incident rays do NOT individually obey Snell's law (eq. 22.4). Nevertheless, Snell's law can be reformulated in terms of components as follows:

$$\tan^2\alpha_2 = b_{\alpha\beta}\cdot\tan^2\alpha_1 \qquad (22.7a)$$

$$\tan^2\beta_2 = b_{\alpha\beta}\cdot\tan^2\beta_1 \qquad (22.7b)$$

where α_2 and β_2 are the components of the refracted ray (analogous to α_1 and β_1), and

$$b_{\alpha\beta} = \frac{\mu_{12}^2}{1+(1-\mu_{12}^2)\cdot\left\{\tan^2\alpha_1+\tan^2\beta_1\right\}} \qquad (22.8)$$

These equations are abbreviated as

$$\alpha_2 = S_\alpha(\alpha_1,\beta_1,,\mu_{12}) = \arctan\left[\left(b_{\alpha\beta}\cdot\tan^2\alpha_1\right)^{1/2}\right] \qquad (22.9b)$$

$$\beta_2 = S_\beta(\alpha_1,\beta_1,,\mu_{12}) = \arctan\left[\left(b_{\alpha\beta}\cdot\tan^2\beta_1\right)^{1/2}\right] \qquad (22.9b)$$

where S represents Snell's law for components.

22.1.3. Huygens' Principle

Huygens suggested that every point along a wave front acts like a generator of new spherical secondary wavelets. Wave-front position after some time interval is located at the tangent to all of the

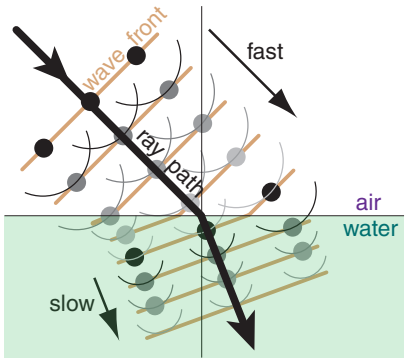

Figure 22.4
Propagation of wave fronts (tan color) across an air-water interface. The wave fronts are analogous to ocean wave crests, and the thick black arrow shows the direction that the waves are moving. This movement direction is called the ray path.

new wavelets. Thus, when a portion of a wave front encounters a medium with a slower light velocity, then that portion of the wave slows, causing the whole wave front to turn into the medium (Fig. 22.4).

22.1.4. Critical Angle

When Snell's law is applied to light rays moving from a denser medium (having slower light velocity) to a less-dense medium (having faster light velocity), there is a **critical angle** at which light is bent so much that it follows the interface. At angles greater than this critical incidence angle, light cannot refract out of the dense medium at all. Instead, all of the light reflects (Fig. 22.5).

The critical angle θ_c is found from:

$$\sin(\theta_c) = \frac{n_2}{n_1} \qquad \bullet(22.10)$$

where n_1 is the refractive index for the incident ray (i.e., in the denser medium with slower light velocity). An example is a light ray moving out of water and into air (i.e., $n_2 < n_1$). For red light the critical angle is about 48.7°, while for violet light the it is about 48.1°. There is no critical angle for light moving into a denser medium (i.e., $n_2 > n_1$).

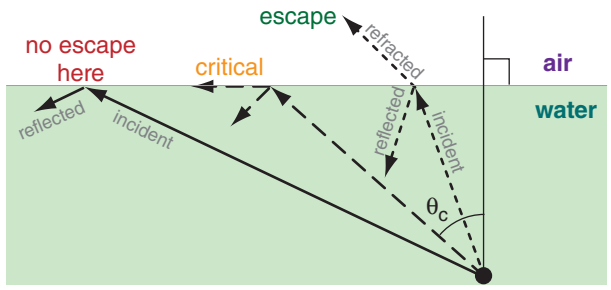

Figure 22.5
When light travels from a dense toward a less-dense medium (e.g., from water to air), angles greater than critical θ_c cannot escape from the denser medium.

Sample Application

Find the critical angle for red light going from a cirrus-cloud ice crystal to air, where the air state is T = –20°C & P = 40 kPa.

Find the Answer

Given: red light λ = 0.7 μm, T = –20°C & P = 40 kPa.
Find: θ_c = ? °

From Table 22-1: n_{ice} = 1.3074 and n_{air} = 1.0001239.
Use eq. (22.10):
θ_c = arcsin(1.0001239/1.3074) = **49.9°**.

Check: Magnitude OK. Units OK.
Exposition: This critical angle is close to that for liquid water, because the refractive indices for liquid and solid water are nearly the same.

22.2. LIQUID-DROP OPTICS

Most raindrop water optics are found by looking away from the sun. **Rainbows** are circles or portions of circles (Fig. 22.6) that are centered on the **antisolar** point, which is the point corresponding to the shadow of your head or camera. (As viewed by the observer, the antisolar point is also called the sun's **antipodal point**.)

Primary rainbows have red on the outside of the circle, and are the brightest and most easily

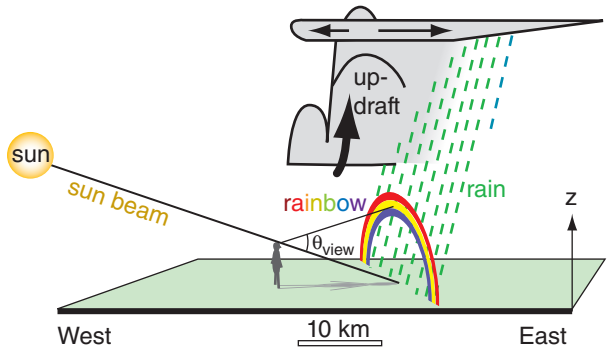

Figure 22.6
Orientation of rainbows relative to the observer and the sun. Look toward your shadow to find the rainbow.

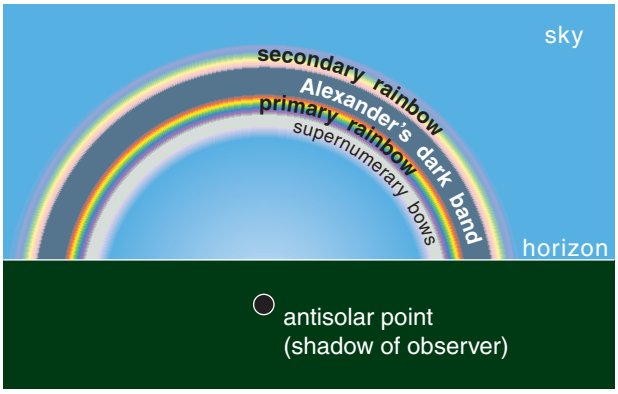

Figure 22.7
Rainbows. The brightest is the primary rainbow, with the red color on the outside of the circle. Secondary and supernumerary bows are fainter, and are often not visible.

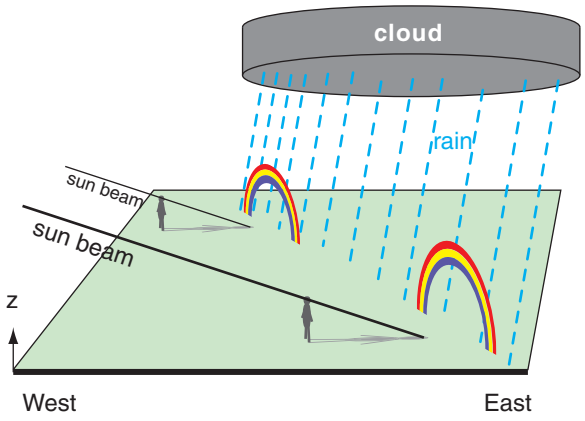

Figure 22.8
Different observers see different rainbows.

seen (Fig. 22.7). The **viewing angle** (θ_{view} = angle between two lines: the line from your eye to the rainbow and the line from your eye to the antisolar point) is about 42°. **Secondary rainbows** have red on the inside at viewing angle of about 50°. **Supernumerary bows** are very faint, and touch the inside of the primary rainbow — these will be discussed in the Diffraction and Interference section.

At any one time for any one rain storm, different observers see different rainbows caused by different light rays interacting with different raindrops (Fig. 22.8). Hence, one observer in a region of bright sun and large drops might see a vivid rainbow, while another observer a half kilometer away might see only a weak or partial rainbow in light rain with smaller drops.

We can explain these rainbow phenomena using geometric optics, assuming spherical raindrops. First, we will consider the portion of incident sunlight that is lost due to reflection off the outside of the drop. Then we will look at the remainder that is refracted and reflected in the drop to make the rainbow.

22.2.1. Reflection from Water

Rays of light that hit a water surface at a shallow angle are reflected more than those hitting straight on. Reflectivity r vs. elevation angle Ψ above the water surface is approximately:

$$r = r_o + r_1 \cdot e^{-\Psi/a} \qquad (22.11)$$

where $r_o = 0.02$, $r_1 = 0.98$, and $a = 9.3°$. This is plotted in Fig. 22.9.

Rays of sunlight can enter a spherical drop at any distance x from the centerline (Fig. 22.10). The ratio of this distance to the drop radius R is called the **impact parameter** (x/R). Because of curvature of the

Sample Application

Just after sunrise, sunlight hits a smooth lake surface at elevation angle 5°. Find the reflectivity.

Find the Answer

Given: $\Psi = 5°$
Find: r = ? (dimensionless)

Use eq. (22.11):
$r = 0.02 + 0.98 \cdot \exp(-5°/9.3°) = \underline{\mathbf{0.59}}$

Check: Units dimensionless. Magnitude agrees with Fig. 22.9.
Exposition: 59% of incident sunshine in this case is reflected away, and is not available to heat the lake.

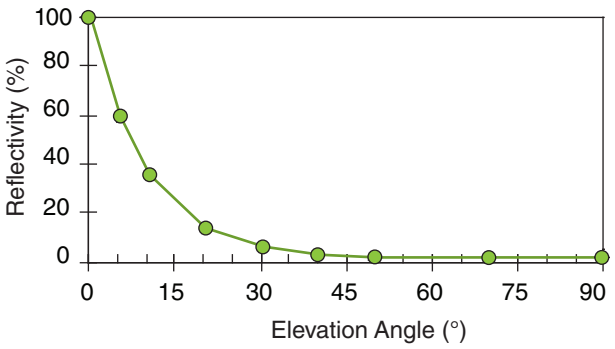

Figure 22.9
Reflectivity from a water surface as a function of ray elevation angle.

Sample Application

For a light ray hitting a spherical raindrop at a distance from the center of 90% of the drop radius, find the elevation angle and the fraction of light reflected.

Find the Answer:
Given: $x/R = 0.9$
Find: Ψ = ?°, and r = ? dimensionless

Use eq. (22.12): $\Psi = \arccos(0.9) = 25.8°$
Use eq. (22.11): $r = 0.02 + 0.98 \cdot \exp(-25.8°/9.3°) = \underline{\mathbf{0.081}}$

Check: Units OK. Magnitude agrees with Fig. 22.9.
Exposition: Even at this large impact parameter, only 8% of the light is reflected off the outside.

drop surface, rays arriving at larger impact parameters strike the drop at smaller elevation angles:

$$\psi = \arccos\left(\frac{x}{R}\right) \qquad \bullet(22.12)$$

Thus, the amount of reflected light from a drop increases with increasing impact parameter.

22.2.2. Primary Rainbow

Rays that are not reflected from the outside of the drop can make zero or more reflections inside the drop before leaving. Those entering rays that make one reflection (in addition to the two refractions during entry and exit) cause the **primary rainbow** (Fig. 22.11). White light is dispersed by the refractions such that reds are bent less and appear on the outside of the rainbow circle, because they come to your eyes from raindrops further from the antisolar point. Violets are bent more and appear on the inside (Fig. 22.12) because the come to your eyes from other drops that are closer to the antisolar point.

Variations of impact parameter cause a range of output viewing angles θ_{view} according to:

$$\theta_{view} = 4 \cdot \arcsin\left(\frac{n_{air}}{n_{water}} \cdot \frac{x}{R}\right) - 2 \cdot \arcsin\left(\frac{x}{R}\right) \qquad \bullet(22.13)$$

where x/R is the impact parameter, and n is refractive index. In other words, there is not a single magic angle of 42° for the primary rainbow. Instead, there is a superposition of many rays of different colors with a wide range of viewing angles.

To learn how these rays interact to form the rainbow, we can solve eq. (22.13) on a spreadsheet for a large number of evenly spaced values of the impact parameter, such as intervals of 0.02 for x/R. Output viewing angles, measured from the antisolar point,

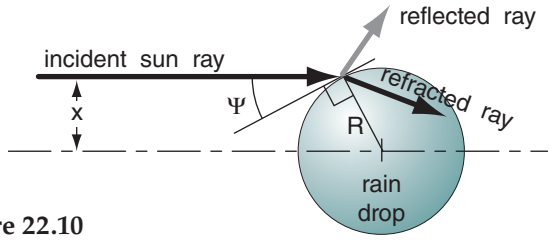

Figure 22.10
Fate of incident ray after first impact with drop.

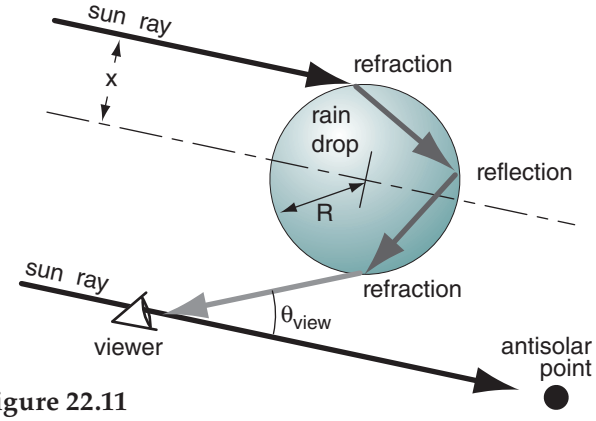

Figure 22.11
Ray geometry for primary rainbow.

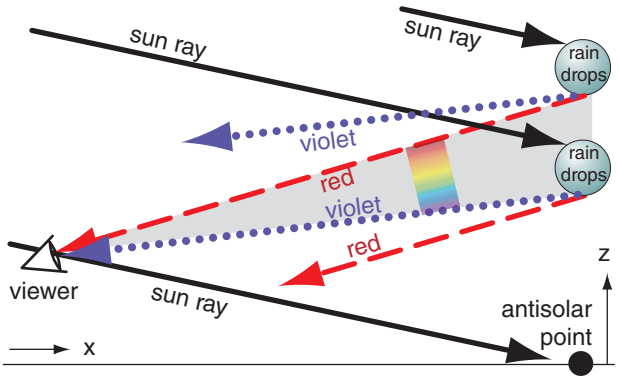

Figure 22.12
Viewer sees primary rainbow (shaded) with red light coming from drops further from the antisolar point than for violet. Thus, the different colors you see come from different drops.

Sample Application

For red light calculate the primary-rainbow viewing angle for x/R= 0.70 in air of P= 80 kPa and T= 0°C.

Find the Answer
Given: $x/R = 0.70$
$n_{air} = 1.0002295$, $n_{water} = 1.3315$ from Table 22-1.
Find: θ_{view} = ?°
Use eq. (22.13) for the primary rainbow:
$\theta_{view} = 4 \cdot \arcsin(0.7512 \cdot 0.70) - 2 \cdot \arcsin(0.70) = \underline{\mathbf{38.05°}}$

Check: Units OK. Physics OK. Agrees with Fig. 22.13.
Exposition: This lights inside the primary rainbow.

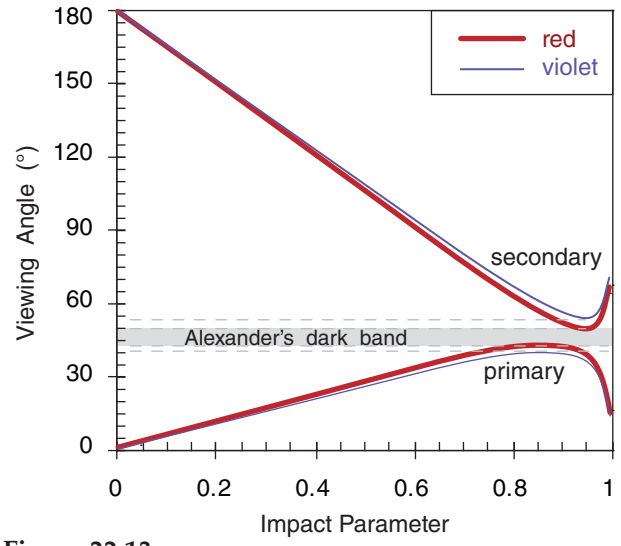

Figure 22.13a
Viewing angles for rainbow rays.

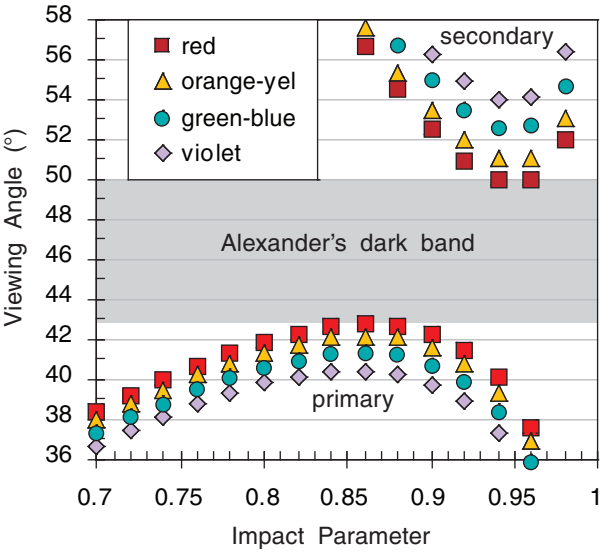

Figure 22.13b
Viewing angles for rainbow rays (enlargement).

Sample Application

For red light calculate the secondary-rainbow viewing angle for x/R= 0.90, with P= 80 kPa and T= 0°C.

Find the Answer

Given: $x/R = 0.90$

$n_{air} = 1.0002295$, $n_{water} = 1.3315$ from Table 22-1.

Find: $\theta_{view} = ?°$

Use eq. (22.14) for the primary rainbow:

$\theta_{view} = 180° + 2\cdot\arcsin(0.90) - 6\cdot\arcsin(0.7512 \cdot 0.90)$

$= \underline{\mathbf{53.09°}}$

Check: Units OK. Physics OK.

Exposition: This almost agrees with Fig. 22.13, which was created for a slightly different T and P.

range between 0° and 42.7°, as plotted in Fig. 22.13a. This is why the sky is brighter inside the primary rainbow (i.e., for viewing angles of 0 to 42.7°), than just outside of it.

Fig. 22.13b is a blow-up of Fig. 22.13a. Three of the data points have a viewing angle of about 42.5°, and these all correspond to rays of red light. Hence, the primary rainbow looks red at that viewing angle. At 42.0°, there are mostly orange-yellow data points, and just a couple red points. Hence, at this angle the rainbow looks orange. Similar arguments explain the other colors. Inside the primary rainbow the sky looks white, because roughly equal amounts of all colors are returned at each viewing angle.

22.2.3. Secondary Rainbow

Entering light rays can also make two reflections before leaving the raindrop, as sketched in Fig. 22.14. The extra reflection reverses the colors, putting red on the inside of the circle of a **secondary rainbow**. At each internal reflection some light is lost (refracted) out of the drop. Thus, the secondary rainbow is faint — only 43% as bright as the primary rainbow.

The relationship between impact parameter and viewing angle for a secondary rainbow is:

•(22.14)

$$\theta_{view} = 180° + 2\cdot\arcsin\left(\frac{x}{R}\right) - 6\cdot\arcsin\left(\frac{n_{air}}{n_{water}}\cdot\frac{x}{R}\right)$$

where x/R is the impact parameter, and n is refractive index. Again, a range of output viewing angles occurs because light enters over the full range of impact parameters. In this case, the sky is dark inside of the secondary rainbow (about 50° viewing angle), and bright outside, as sketched in Figs. 22.13a & b, based on spreadsheet calculations.

Higher-order rainbows (having more internal reflections) are theoretically possible, but are rarely seen because they are so faint:

- **Tertiary Rainbow**:
  3 internal reflections
  θ_{view} = 137.52°
  intensity ≈ 24% as bright as the primary
- **Quaternary Rainbow**:
  4 internal reflections
  θ_{view} = 137.24°
  intensity ≈ 15% as bright as the primary
- **5th Order Rainbow**:
  5 internal reflections
  θ_{view} = 52.9°
  very faint

Viewing angles for tertiary and quaternary rainbows are 43° from the sun (i.e., not from the antisolar point). Hence, their faint presence is washed out by the intense zero-order glow from the sun. **Zero-or-**

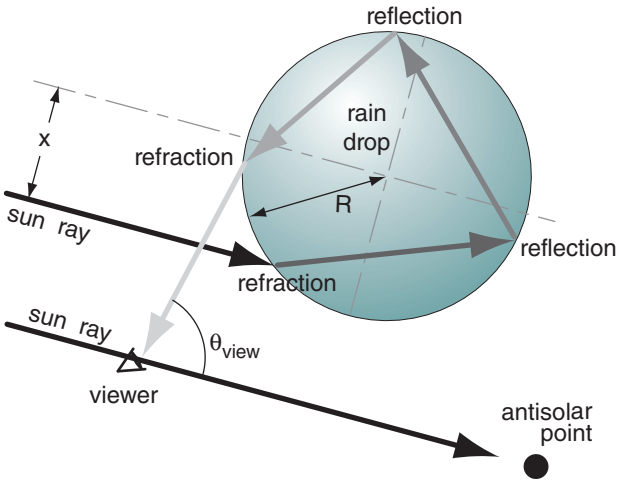

Figure 22.14
Ray geometry for secondary rainbow.

der glow is light from the sun passing through a raindrop with no internal reflections while en route to the observer.

22.2.4. Alexander's Dark Band

Neither the primary nor secondary rainbows return light in the viewing-angle range between 42.7° and 50°. Hence, the sky is noticeably darker between these rainbows (Figs. 22.7 & 22.13). This dark region is called **Alexander's dark band**, after Greek philosopher Alexander of Aphrodisias who described it during the third century A.D.

22.2.5. Other Rainbow Phenomena

Larger-diameter raindrops cause more vivid, colorful rainbows. But as discussed in the Satellite & Radar chapter, large raindrops are often not spherical. A mixture of large non-spherical drops (oblate spheroids the shape of hamburger buns) and moderate-sized spherical drops causes cause **twinned rainbows**, where the top of the rainbow circle splits into two rainbows (Fig. 22.15a).

Sea-spray rainbows are about 0.8° smaller radius than normal rainbows, because of greater refraction by salt water. Near sunset, the blue-diminished sunlight illuminates raindrops with reddish light, creating **red bows** with enhanced red and orange bands. Faint rainbows (**moon bows**) can also be created by moonlight at night.

Reflection rainbows form when the incident sunlight bounces off a lake before hitting the raindrops (Fig. 22.15b). This bow is centered on the **anthelic point**, which is as high above the horizon as the antisolar point is below, but at the same azimuth.

INFO • Rainbows and the Renaissance

German monk Theodoric von Freiberg created a physical model of rainbow physics in 1304 by filling a glass sphere with water. By carefully shining light through it at different impact parameter values, he could measure the various output angles. However, the physics behind these observations were not explained until the renaissance, after Willebrod Snell van Royen had discovered the law for refraction in the early 1600's.

Twenty years after Snell's discovery, Descartes used it to demonstrate the capabilities of his scientific method by mathematically solving the rainbow problem. His calculations were very similar to our spreadsheet calculations, except that he manually performed calculations for a large number of different impact parameters. Through these repetitive "brute-force" calculations he verified the magic number of 42° for the brightest returned light, and 50° for the secondary rainbow.

About 30 years later, Newton applied his knowledge of color dispersion to explain why the rainbow has colors. Also, he was able to use his invention of calculus to elegantly derive the magic angle of 42°.

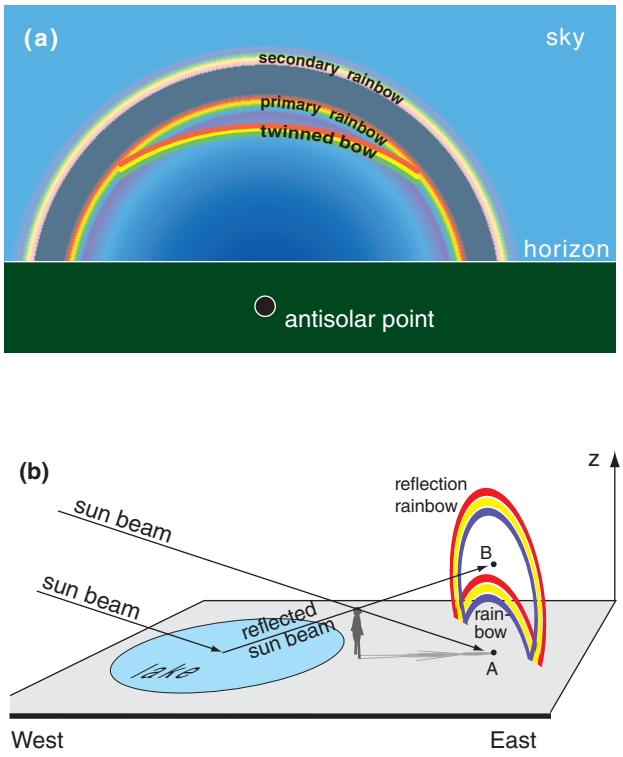

Figure 22.15
(a) Twinned primary rainbow (twinned bow) inside the normal primary rainbow, caused by large oblate raindrops. (b) Reflection rainbow caused by sunlight reflecting from a smooth lake surface or waveless ocean before reaching the falling raindrops. The reflection bow is a circle centered on the anthelic point (B), while the normal primary rainbow circle is centered on the antisolar point (A).

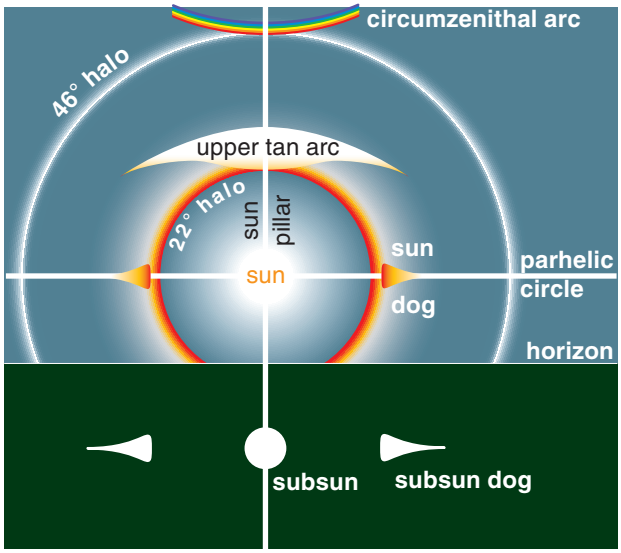

Figure 22.16
Some of the more common halos and other optical phenomena associated with ice crystals in air.

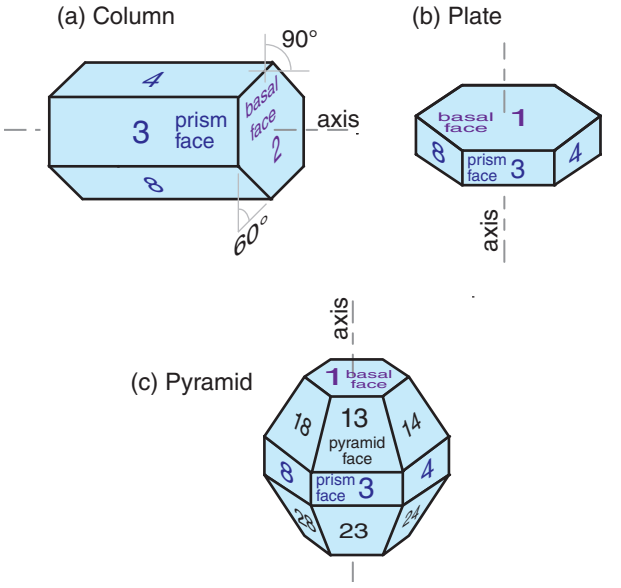

Figure 22.17
Ice-crystal geometry relevant to atmospheric optics. The angles highlighted in (a) are known as **wedge angles**, β_c, *which correspond to the angles of a prism that would yield the refraction as discussed in this section. There are many different wedge angles (not shown here) between different faces of the pyramid.*

22.3. ICE CRYSTAL OPTICS

Most of the common ice-crystal optical phenomena are seen by looking more-or-less toward the sun (Fig. 22.16). To observe them, shield your eyes from the direct rays of the sun to avoid blinding yourself. Also, wear sunglasses so your eyes are not dazzled by the bright sky close to the sun.

Subsuns, sun pillars, and parhelic circles are caused by simple reflection from the outside surface of ice crystals. Reflections from inside the ice crystal can also contribute to the intensity of these phenomena.

Sundogs, halos, circumzenithal arcs, and tangent arcs are caused by refraction through the ice crystals, with the red color closest to the sun.

Subsun dogs are caused by both refraction and reflection in the ice. There are many other optical phenomena related to ice crystals, only a few of which we cover here.

Ice crystals (types of snow) can form as high-altitude cirrus clouds, can be naturally seeded within and fall from the base of mid-altitude water-droplet clouds, can grow within low- or mid-altitude cloudless cold air of high relative humidity, or can be stirred up by the wind from fresh surface snow. For all these situations, the best optical displays occur with a diffuse concentration of crystals in the air. Namely, the air looks mostly or partially clear, except for sparkles of light reflected from the sparsely spaced crystals (nicknamed **diamond dust**).

The crystals have a variety of shapes, most with hexagonal cross-section (see Figs. 7.12 and 7.13 in the Precipitation chapter). The two shapes most important for atmospheric optical phenomena are the **hexagonal column** and **hexagonal plate** (Fig. 22.17). The plate is just a very short column. **Hexagonal pyramid**-capped columns cause rarer halos.

Plates or columns, if larger than about 30 μm, gently fall through the air with the **orientation** relative to horizontal as sketched in Fig. 22.17. Namely, the crystal axis of large columns is nearly parallel to the ground, and the axis of large plates is nearly vertical. Surprisingly, this natural orientation is associated with relatively high aerodynamic drag on the falling crystal. Smaller crystals tend to tumble as they fall, giving random orientations.

Crystal faces are numbered as shown in Fig. 22.17, where **basal faces** numbered 1 and 2 mark the ends of the hexagonal column, and **prism faces** 3 - 8 wrap sequentially around the sides. In naming the relative positions of prism faces: 4 and 3 are examples of **adjacent** faces, 4 and 8 are **alternate** faces, while 4 and 7 are **opposite** faces. **Pyramid faces** are numbered as double digits, where the first

digit indicates the number of the adjacent basal face, and the second digit indicates the number of the adjacent prism face. The numbering is useful to track ray paths.

As shown in Fig. 22.17, the most important **wedge angles** (β_c) of plate and column crystals are 60° (such as between faces 3 and 7, or 4 and 8) and 90° (such as between faces 3 and 1, or between 4 and 2). Angles for pyramids are discussed later.

22.3.1. Sun Pillar

A sun pillar is a vertical column of light that appears to come out of the top (and sometimes the bottom) of the sun (Fig. 22.16). It forms when sunlight reflects off the outside of any of the following nearly-horizontal faces:

- prism faces of large oriented column ice crystals (such as off of face 8 in Fig. 22.18a),
- basal faces of fluttering large oriented plates (such as off face 2 in Fig. 22.18b), or
- basal faces of large oriented **dendrites** (6-armed snowflake plates) (such as off the bottom of the snowflake in Fig. 22.18d).

These crystals act like myriad tiny mirrors.

Internal reflections can contribute to the intensity of sun pillars. In the example of Fig. 22.18c, light enters the ice crystal (with refraction) through face 5, then reflects from the inside of the crystal at face 1, and leaves (with refraction) from face 8.

An end view of this phenomenon for reflection from oriented hexagonal columns is sketched in Fig. 22.19. Column crystals are free to rotate about their column axis as they gently fall to Earth, and flat plates and dendrites have random wobble of their axes causing them to flutter like leaves when they fall. As a result, some of the ice crystals have faces that by chance reflect the sunlight to your eye, while other ice crystals reflect the sunlight elsewhere.

Relatively few sunbeams reflect to your eye, causing the sun pillar to be very faint. The best time to observe sun pillars is at sunrise or sunset when the sun is hidden just below the horizon, but is still able to illuminate the ice precipitation. Sun pillars often appear to be red not because of refraction in the crystal, but because light from the rising or setting sun has lost much of its blue components due to scattering from air molecules before it reaches the ice crystals.

Similar pillars can form above and below:

- bright street lights,
- the moon and bright planets (e.g., Venus), and
- other bright lights, such as aircraft lights.

These pillars often have the same color as the light source.

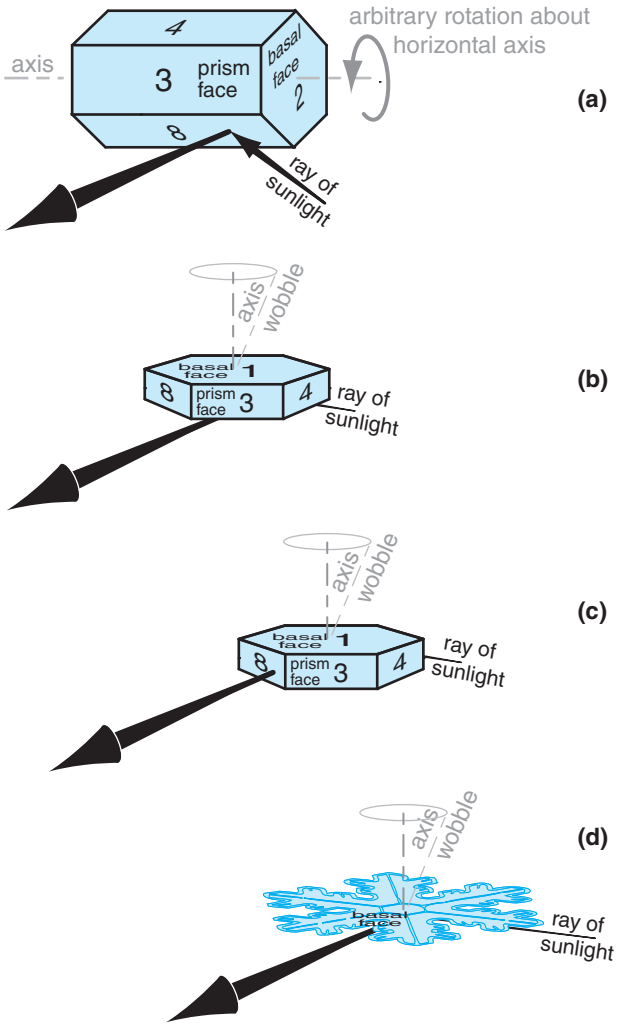

Figure 22.18
Sun-pillar optics caused by reflection of sunlight off the faces of large (a) ice columns with their axes orientated horizontally, (b & c) vertically-oriented plates, and (d) oriented dendrites.

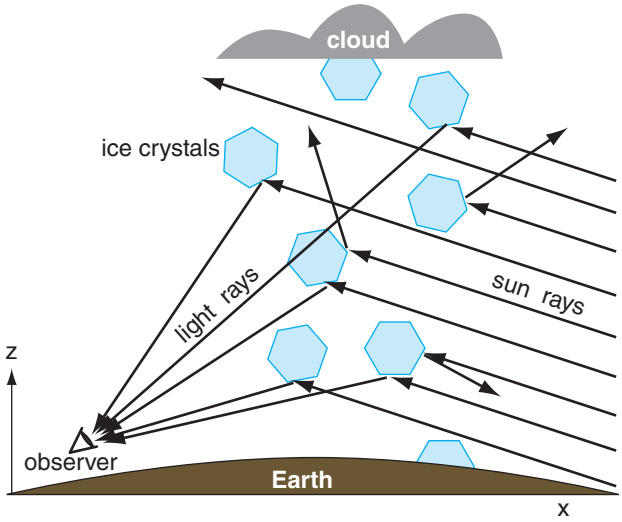

Figure 22.19
Geometry of sun-pillar optics (end view) reflecting from oriented large hexagonal-column ice crystals (size is exaggerated).

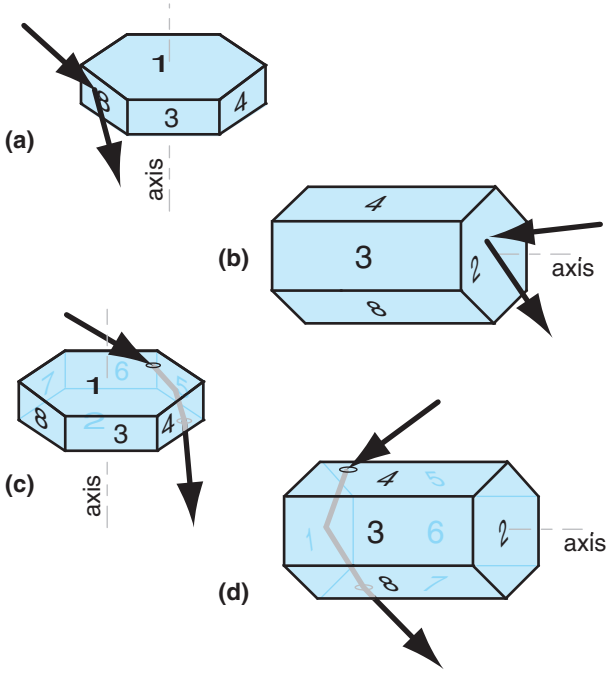

Figure 22.20
Ray geometry of parhelic-circle optics, showing some of the possible external and internal reflections. Small ovals indicate points where light rays enter or leave the ice crystal.

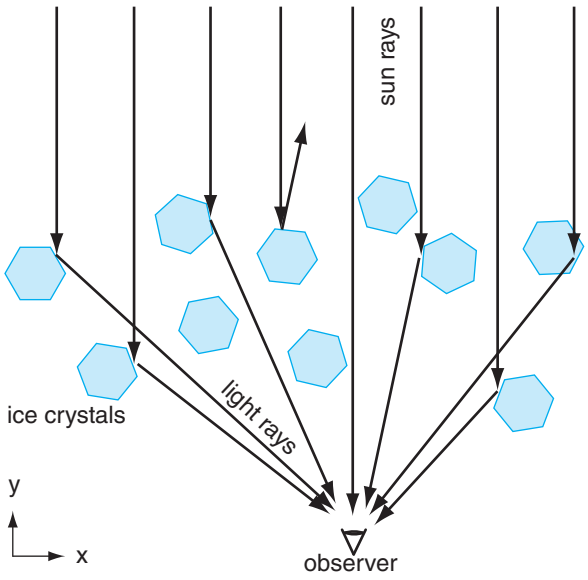

Figure 22.21
Reflection from many large hexagonal plates (size is exaggerated) to form a parhelic circle (top or plan view).

22.3.2. Parhelic Circle

The parhelic circle is a horizontal band of white light extending left and right through the sun (Fig. 22.16). It can be formed by external reflection off of the vertical faces of large hexagonal plates (e.g., face 8 in Fig. 22.20a) or large hexagonal columns (e.g., face 2 in Fig. 22.20b). It can also be formed by internal reflection off of similar vertical faces, such as the ray path touching faces 1-5-2 in Fig. 22.20c, or the path touching faces 4-1-7 in Fig. 22.20d.

These crystals can have any rotation orientation about their axis, causing reflections from many different ice crystals to reach your eye from many different angles left and right from the sun (Fig. 22.21). In other words, they act as a large number of small mirrors.

22.3.3. Subsun

The subsun is a spot of white light seen below the horizon (Fig. 22.16), as viewed looking down from a bridge, mountain, or aircraft. It forms by external reflection of sunlight off of the top surfaces of large hexagonal plates (face 1 in Fig. 22.22a), and by internal reflection (face 2 in Fig. 22.22b; namely, the ray touches faces 7-2-4). If all the hexagonal plates are oriented horizontally, they act as mirrors to produce a simple reflection of the sun (Fig. 22.23). As given by eq. (22.1), the subsun appears the same angle θ_3 below the horizon that the sun is above θ_1.

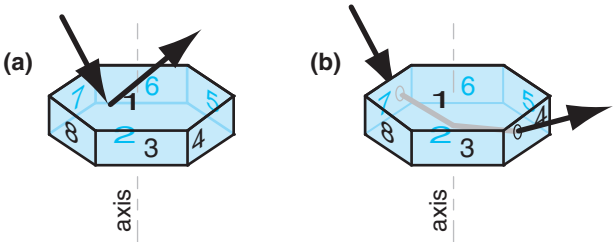

Figure 22.22
Ray geometry of subsun optics. Small ovals indicate points where light rays enter or leave the ice crystal.

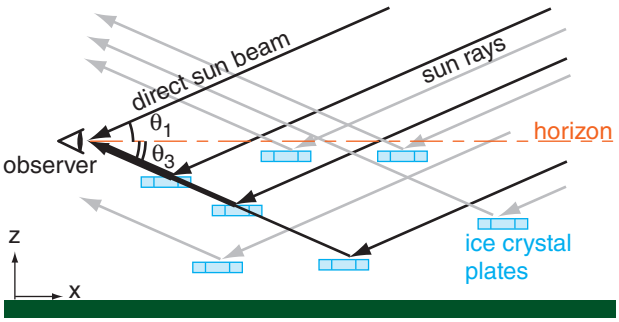

Figure 22.23
Reflection from many ice-crystal plates to form a subsun (side view). Grey rays reach someone else's eyes.

22.3.4. 22° Halo

Optics for 22° halos (Fig. 22.16) are not as simple as might be expected. Small ice-crystal columns are free to tumble in all directions. As a result, light rays can enter the crystal at a wide range of angles, and can be refracted over a wide range of sky.

The brightest light that we identify as the halo is caused by refraction through those ice crystals that happen to be oriented with their column axis perpendicular to the sun rays (Fig. 22.24). We will study this special case. Different crystals can nevertheless have different rotation angles about their axis (the dark point in the center of the ice crystal of Fig. 22.24). As a result, the angle of incidence θ_1 can vary from crystal to crystal, thereby causing different viewing (output) angle θ_2 values.

For hexagonal crystals (for which the **wedge angle** is $\beta_c = 60°$) and for the special case of light rays approaching normal to the column axis, Snell's law yields:

$$\theta_2 = \theta_1 - \beta_c + \arcsin\left\{\frac{n_{ice}}{n_{air}} \cdot \sin\left[\beta_c - \arcsin\left(\frac{n_{air}}{n_{ice}} \cdot \sin\theta_1\right)\right]\right\} \quad \bullet(22.15)$$

where n is refractive index.

The 22° halo observed by a person is the result of superposition of rays of light from many ice crystals possessing many different rotation angles. Hence, it is not obvious why 22° is a magic number for θ_2. Also, if refraction is involved, then why are the red to yellow colors seen most vividly, while the blues and violets are fading to white?

To answer these questions, suppose ice crystals are randomly rotated about their axes. There would be an equal chance of finding an ice crystal having any incidence angle θ_1. We can simulate this on a computer spreadsheet by doing calculations for a large number of evenly-spaced incidence angles (for example, every 2°), and then calculating the set of θ_2 angles as an outcome. The result is plotted in Fig. 22.25 for two of the colors (because n_{air}/n_{ice} varies with color).

Colors and angles of a 22° halo can be explained using Fig. 22.26 (which is a zoomed view of Fig. 22.25). For viewing (output) angles less than about 21.6°, there is no refracted light of any color; hence, the halo is dark inside (the edge closest to the sun).

In the range of viewing angles averaging 22° (i.e., from 21.6° to 22.6°), there are 29 data points plotted in Fig. 22.26, which cause the bright ring of light we call the halo. There are also data points at larger angles, but they are more sparse — causing the brightness of the halo to gradually fade at greater viewing angles from the sun.

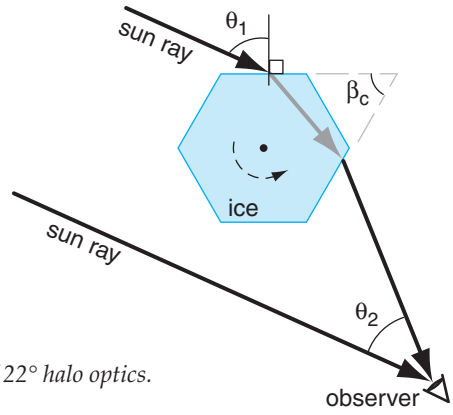

Figure 22.24
Ray geometry of 22° halo optics.

Sample Application

What is θ_2 if $\theta_1 = 80°$ and $\beta_c = 60°$ for red light in a 22° halo? $T = -20°C$, $P = 80$ kPa, $RH = 75\%$.

Find the Answer

Given: $\theta_1 = 80°$. $\beta_c = 60°$. $\lambda = 0.7$ μm for red light.
$n_{air} = 1.0002479$, $n_{ice} = 1.3074$ from Table 22-1.
Find: $\theta_2 = ?°$

Use eq. (22.15) with $\beta_c = 60°$ for hexagonal crystal:

$$\theta_2 = 80° - 60° + \text{asin}\left\{\frac{1.3074}{1.0002479} \cdot \sin\left[60° - \text{asin}\left(\frac{1.0002479}{1.3074} \cdot \sin 80°\right)\right]\right\}$$

$$= 80° - 60° + 14.59° = \underline{\mathbf{34.59°}}$$

Check: Units OK. Physics OK.
Exposition: Quite different from 22°, but agrees with Fig. 22.25. Namely, this is one of the light rays that contributes to the bright glow outside the 22° halo, as sketched in Fig. 22.16.

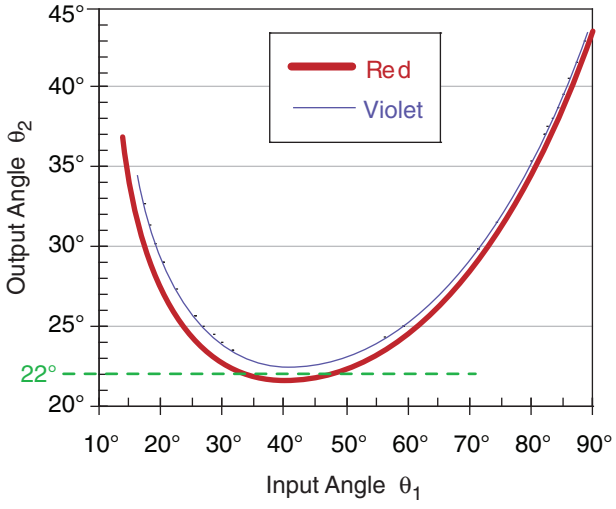

Figure 22.25
Viewing (output) angles θ_2 from hexagonal ice crystals in a 22° halo, for various incident angles θ_1 of sunlight.

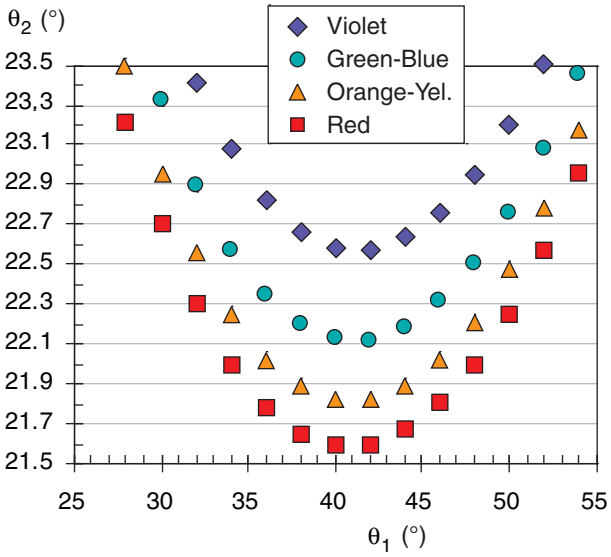

Figure 22.26
Blow-up of viewing (output) angles θ_2 from hexagonal ice crystals in a 22° halo, for various incident angles θ_1.

Sample Application
Find θ_{2min} for green-blue light for wedge angle 60°.

Find the Answer
Given: $\beta_c = 60°$, $n_{ice} = 1.3135$ for blue-green (λ=0.5 μm).
Find: $\theta_{2min} = ?\,°$. (Assume $T = -20°C$ & $n_{air} \approx 1.0$.)

Use eq. (22.16): $\theta_{2min} = 2 \cdot \arcsin[1.3135 \cdot \sin(30°)] - 60°$
$= 82.10° - 60° = \underline{\mathbf{22.10°}}$

Check: Agrees with Table 22-2.
Exposition: The different colors of the 22° halo are not all at exactly 22°.
CAUTION: If you do these angle calculations on a spreadsheet, don't forget to convert to/from radians for the sine/arcsine terms.

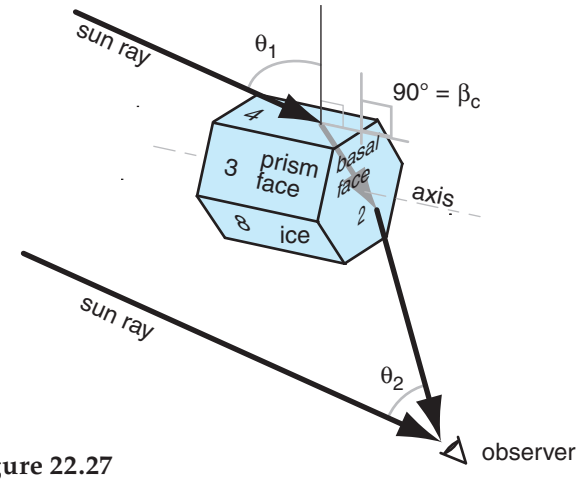

Figure 22.27
Ray geometry for a 46° halo.

For a viewing angle range of $\theta_2 = 21.5°$ to 21.7°, we see four "red light" data points in Fig. 22.26, but no other colors. Thus, the portion of the halo closest to the sun looks bright red. In the next range of viewing angles (21.7° - 21.9°), we see four "yellow-orange" and two "red" data points. Thus, in this range of viewing angles we see bright orange light.

In the angle range 22.1 - 22.3°, there are four blue-green data points, and two orange-yellows and two reds. These colors combine to make a bluish white color. By an angle of 23° , there are roughly equal portions of all colors, creating white light. Thus, the colors of a 22° halo can have bright reds, oranges, and yellows on the inside, fading to light green and bluish-white further away from the sun.

The **minimum viewing angle** is the angle for which the halo gets its name, and can be found from:

$$\theta_{2\,min} = 2 \cdot \arcsin\left[\frac{n_{ice}}{n_{air}} \cdot \sin\left(\frac{\beta_c}{2}\right)\right] - \beta_c \qquad (22.16)$$

where β_c is wedge angle and n is refractive index. This is at the bottom of the curves in Fig. 22.26.

22.3.5. 46° Halo

The 46° halo (Fig. 22.16) forms by sun rays shining through a prism face and a basal end of short hexagonal columns (Fig. 22.27). Equations (22.15 and 22.16) apply, but with an ice wedge angle β_c = 90°. The resulting viewing angles θ_2 are shown in Fig. 22.28 for a variety of input angles θ_1. Except for the different radius, this halo has visual characteristics similar to those of the 22° halo. But it is faint, and less frequently seen.

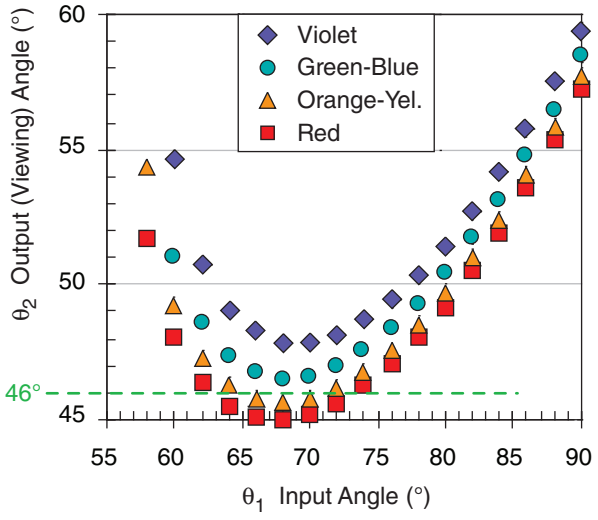

Figure 22.28
Viewing (output) angles for a 46° halo.

Sample Application

Find the viewing angle θ_2 for a 46° halo, given input angle $\theta_1 = 80°$ and $\beta_c = 90°$ for red light.

Find the Answer

Given: $\theta_1 = 80°$, $\beta_c = 90°$. $\lambda = 0.7$ μm for red light.
Find: $\theta_2 = ?°$
Assume: $n_{air} = 1.0002479$, $n_{ice} = 1.3074$ from Table 22-1.

Use eq. (22.15):
$$\theta_2 = 80° - 90° + \text{asin}\left\{\frac{1.3074 \cdot \sin}{1.0002479}\left[90° - \text{asin}\left(\frac{1.0002479}{1.3074} \cdot \sin 80°\right)\right]\right\}$$
$$= \underline{\mathbf{49.25°}}$$

Check: Units OK. Physics OK.
Exposition: This agrees with Fig. 22.28.

22.3.6. Halos Associated with Pyramid Crystals

Ice crystals with pyramid ends (Fig. 22.17c) have a wide variety of wedge angles depending on the path of the light ray through the crystal. This can cause additional halos of differing radii centered on the sun (Fig. 22.29).

Table 22-2 lists the ray path, wedge angle, and minimum viewing angle (from eq. 22.16) for some of these odd-radius halos. The 9° halo is often hard to see against the glare close to the sun, while the 18°, 20°, 23°, and 24° halos might be mis-reported as 22° halos unless accurate measurements are made. Nonetheless, most of the rare halos have been observed and photographed.

Table 22-2. Halo viewing angles (θ_{2min}) found from eq. (22.16). Ray paths refer to the face numbers in the Fig. at right. β_c = wedge angle of ice crystal (from *W. Tape & J. Moilanen, 2006: "Atm. Halos & the Search for Angle x"*. $n_{air} \approx 1.0$

	color =	red	yellow orange	green blue	violet
	wavelength (μm) =	0.7	0.6	0.5	0.4
	(For T = –20°C) n_{ice} =	1.3074	1.3099	1.3135	1.3199
Halo Name	β_c (°)	Ray Path	Minimum **Halo Viewing Angles** (°)			
9°	25	18 · 5	8.88	8.95	9.06	9.24
18°	52.4	18 · 24	18.11	18.27	18.49	18.89
20°	56	18 · 15	19.73	19.90	20.14	20.58
22°	60	8 · 4	21.64	21.83	22.10	22.59
23°	62	18 · 7	22.65	22.85	23.14	23.66
24°	63.8	18 · 4	23.60	23.81	24.11	24.65
35°	80.2	18 · 14	34.53	34.87	35.37	36.26
46°	90	1 · 3	45.18	45.71	46.49	47.91

Science Graffito

"The skipper he stood beside the helm,
His pipe was in his mouth,
And he watched how the veering flaw did blow
The smoke now West, now South.
Then up and spake an old Sailor
Had sailed to the Spanish Main,
'I pray thee, put into yonder port,
For I fear a Hurricane.
Last night **the moon had a golden ring**,
And tonight no moon we see!'
The skipper he blew a whiff from his pipe,
And a scornful laugh laughed he."
– by Henry Wadsworth Longfellow, from
The Wreck of the Hesperus.

INFO • Estimating 22° Angles

For most people, if you extend your arm fully and open your hand as widely as possible, then the angle that you see subtended by your hand is about 22°. This works for people of different sizes, because hand size and arm length are often proportional.

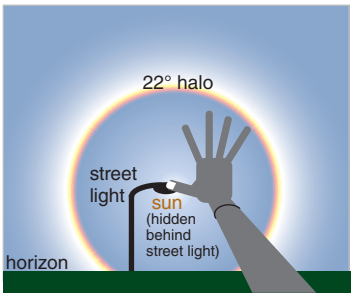

Fig. 22.a

To view halos, first move so that the sun is hidden behind an obstacle such as a street light, stop sign, or a corner of a building, so you don't blind yourself. Then extend your arm and stretch your hand, and position the tip of your thumb over the location where the center of the sun would be (hidden behind the obstacle). The tip of your little finger should just touch the halo if it is indeed a 22° halo.

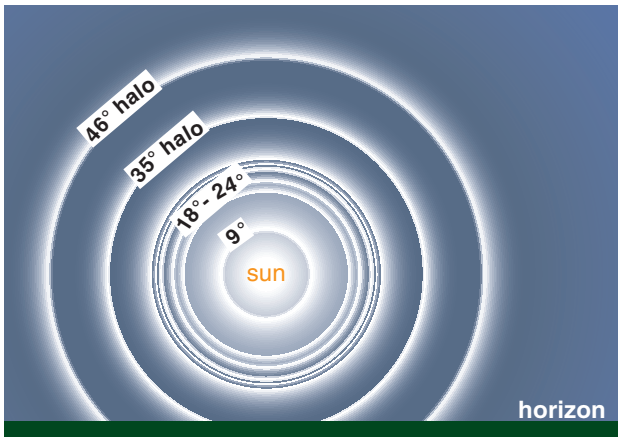

Figure 22.29
Halos. (It is unusual to see all these halos at the same time.)

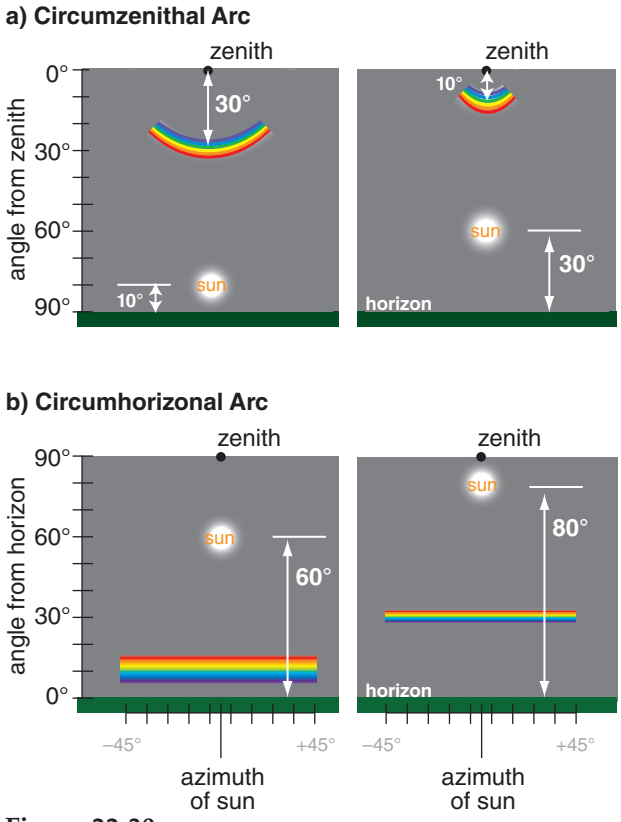

Figure 22.30
Although both circumzenithal and circumhorizontal arcs are portions of circles around the zenith and both are parallel to the horizon, we perceive them differently. Circumzenithal arcs look like a part of a circle around the zenith point, as sketched in (a). Circumhorizontal arcs look like horizontal lines just above the horizon, as sketched in (b). Angles above are approximate.

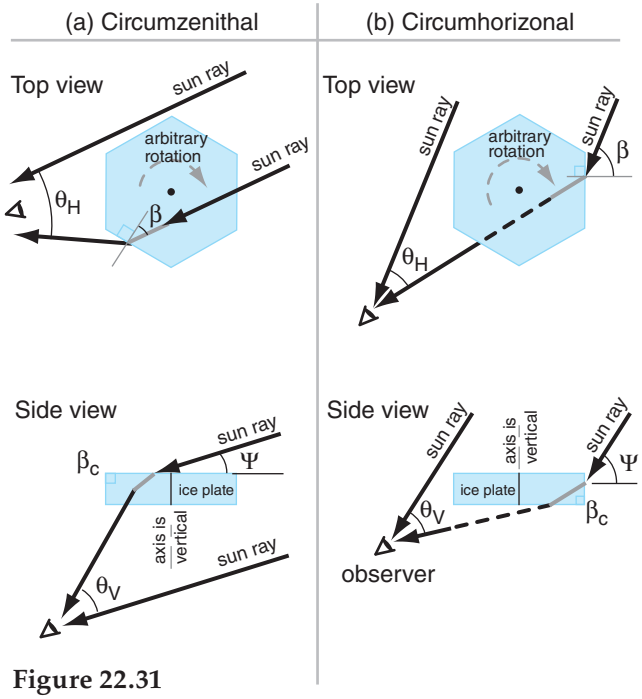

Figure 22.31
Ray geometry for (a) circumzenithal and (b) circumhorizontal arcs.

22.3.7. Circumzenithal & Circumhorizontal Arcs

Circumzenithal arcs and circumhorizontal arcs are similar (Fig. 22.30). They are both portions of circles at constant viewing angle above the horizon, and thus at constant viewing angle from the zenith (the point directly above the viewer). They are lines parallel to the horizon that partially encircle the viewer. Only the portion of the circle within about ±45° azimuth of the sun's azimuth from the viewer are visible; hence, they are seen as arcs, not circles.

Both arcs are caused by light refracted through the $\beta_c = 90°$ wedge angle of large oriented hexagonal plates (Fig. 22.31). For circumzenithal arcs the light ray enters the top of the plate (through basal face 1) and exits through the side (such as through prism face 8 in Fig. 22.17b). For circumhorizontal arcs the ray enters a side (such as face 5) and exits the bottom (face 2). Because refraction is involved, these arcs can be colorful, with red closest to the sun.

The arc's viewing angle from the zenith (i.e., the apparent radius of the arc) varies with solar elevation (Fig. 22.32). The circumzenithal arc is seen high in the sky (above the sun) only when the sun is low in the sky (for solar elevation angles of $0° < \Psi < 32°$). The circumzenithal arc is always outside the 46° halo (Fig. 22.16).

The circumhorizontal arc is seen low in the sky (below the sun) only when the sun is high in the sky ($58° < \Psi \leq 90°$). At high latitudes the circumhorizontal arc is never visible because the sun never gets high enough in the sky.

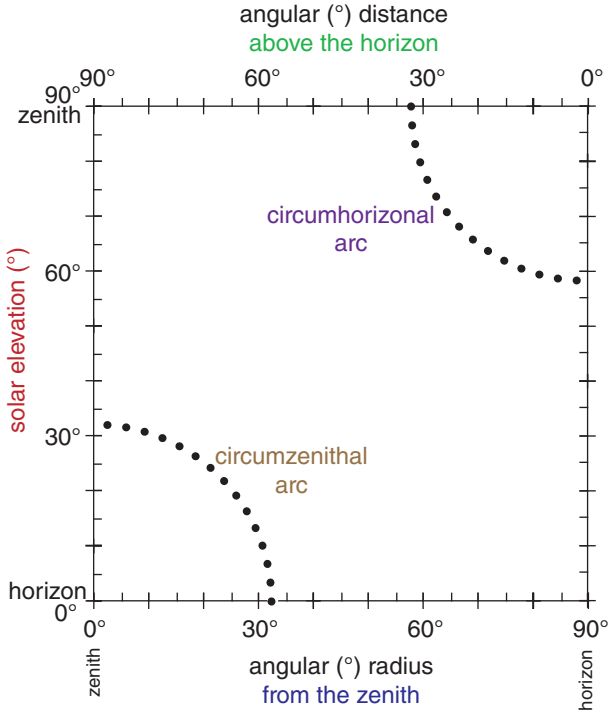

Figure 22.32
Radius of circumzenithal and circumhorizontal arcs about the zenith point, as viewed from the ground.

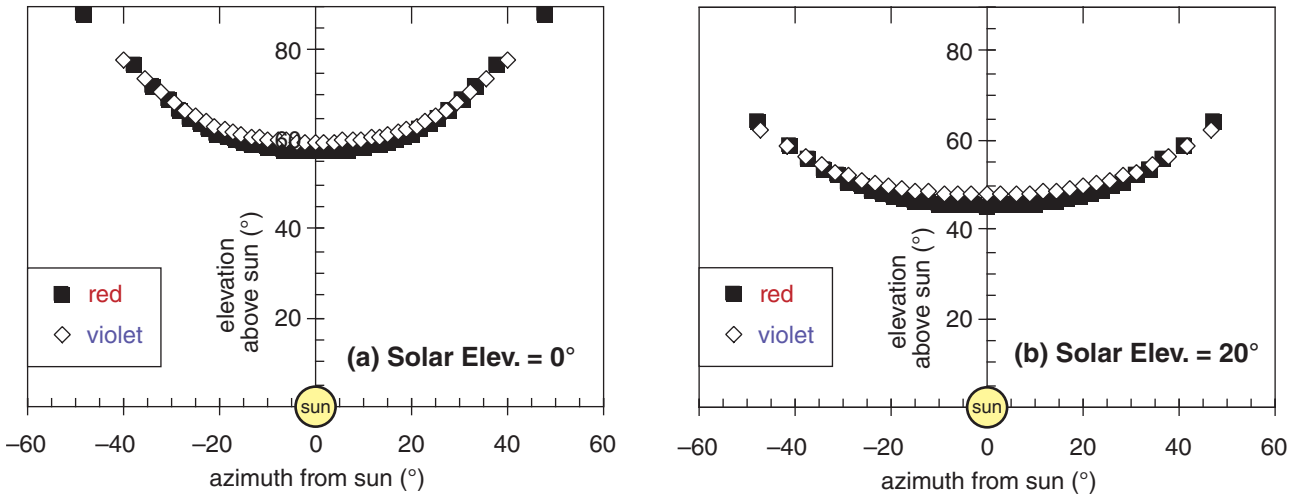

Figure 22.33
Circumzenithal arcs found by solving eq. (22.17) for a variety of crystal rotation angles β, at solar elevation angles of (a) 0°, at left, and (b) 20°, above.

To illustrate how these arcs form, we will focus on just one of them — the circumzenithal arc. The large hexagonal plates can assume any rotation angle β about their vertically-oriented column axis. At different times and locations, there are different solar elevation angles ψ. The ray equations for vertical viewing angle θ_V (elevation above the sun) and horizontal angle θ_H (azimuth from the sun) are:

$$\theta_V = S_\alpha[\arccos(\mu_{ai}\cdot\cos\psi),\beta,\mu_{ia}] - \psi \qquad (22.17)$$

$$\theta_H = S_\beta[\arccos(\mu_{ai}\cdot\cos\psi),\beta,\mu_{ia}] - \beta$$

Subscripts "*ai*" are for rays going from air to ice (e.g., $\mu_{ai} = n_{air}/n_{ice}$), while subscripts "*ia*" are from ice to air (e.g., $\mu_{ia} = n_{ice}/n_{air}$).

A spreadsheet can be used with a large number of evenly spaced values of β to simulate the superposition of rays from a large number of randomly-rotated ice plates. The resulting locus of output viewing angles traces the circumzenithal arc in Fig. 22.33.

Eq. (22.17) does not account for some ray paths that might reflect from the outside of the crystal instead of entering, nor does it include the critical angle for rays already inside the crystal. Thus, some of the points plotted in Fig. 22.33 might not be possible, because the sun rays corresponding to those points either cannot enter the crystal, or cannot leave it.

Science Graffito

"It is clear and cold... And all about is snow and silence. And in the sky are three suns, and all the air is flashing with the dust of diamonds."
– Jack London, on a trip down the Yukon River in search of gold in Alaska.

Sample Application

For a circumzenithal arc, what are the elevation and azimuth viewing angles (relative to the sun)? Solar elevation is 10°. Rotation angle is β = 20°. Assume nearly red light with: $n_{air} = 1.0002753$ and $n_{ice} = 1.307$.

Find the Answer

Given: Ψ = 10°, β = 20°, $n_{air} = 1.0002753$, $n_{ice} = 1.307$
Find: θ_V = ?°, and θ_H = ?°

First, find the refraction parameters:
$\mu_{ai} = n_{air}/n_{ice} = 0.7653$, and $\mu_{ia} = 1/\mu_{ai} = 1.3067$

Next: $\arccos[\mu_{ai}\cos(\Psi)] = \arccos(0.7653\cdot\cos 10°) = 41.09°$

Then, use eqs. (22.17):
$\theta_V = S_\alpha[41.09°,\ 20°,\ 1.3067] - 10°$
$\theta_H = S_\beta[41.09°,\ 20°,\ 1.3067] - 20°$.

To find the *S* values, we first need to use eq. (22.8):

$$b_{\alpha\beta} = \frac{(1.3067)^2}{1+[1-(1.3067)^2]\cdot\left\{[\tan(41.09°)]^2+[\tan(20°)]^2\right\}} = 4.634$$

Then use eq. (22.9):

$$S_\alpha(\alpha_1,\beta_1,,\mu_{12}) = \arctan\left[\left\{4.634\cdot[\tan(41.09)]^2\right\}^{1/2}\right]$$

$S_\alpha = 61.95°$

Similarly: $S_\beta = 38.08°$
Finally: $\theta_V = 61.95° - 10° = \underline{\mathbf{51.95°}}$
$\theta_H = 38.08° - 20° = \underline{\mathbf{18.08°}}$

Check: Units OK. Physics OK.
Exposition: This answer agrees with Fig. 22.33b. Obviously this calculation is tedious for more than one ray, but it is easy on a spreadsheet.

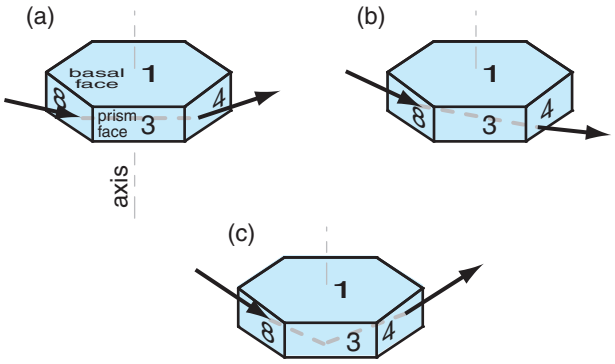

Figure 22.34
Geometry of sun dog optics (oblique side view), for (a) low sun elevation angle, (b) higher sun angle, and for (c) subsun dogs.

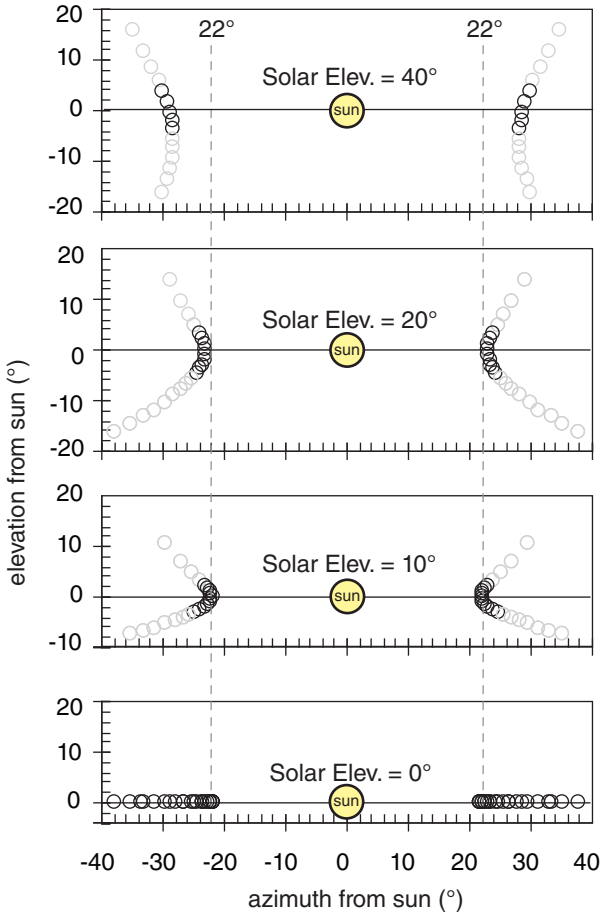

Figure 22.35
Variation of parhelia (sun-dog) appearance with solar elevation angle. Vertical dashed lines are 22° from sun. Greater density of data points indicates brighter parhelia. Grey data points, although solutions to eqs. (22.18), are unphysical because those equations don't consider the finite size of the ice crystals.

22.3.8. Sun Dogs (Parhelia)

Parhelia are bright spots of light to the right and left of the sun, roughly 22° from the sun (Fig. 22.16). As the sun moves through the sky, the parhelia move with the sun as faithful companions — earning their nickname **sun dogs**.

They are formed when light shines through the sides (prism faces) of large horizontal ice-crystal plates that gently fall through the air with their column axes vertical. The crystals are free to rotate about their column axes, so there is no favored rotation angle.

Because of the preferred orientation of the column axis, sun-dog optics depend on the solar elevation angle. When the sun is on the horizon, sun rays shine through the crystal as sketched in Fig. 22.34a, with a nearly horizontal path through prism faces such as 8-4. This causes the parhelia at a viewing angle of 22° from the sun. If a 22° halo is also present due to other smaller ice crystals in the air, then each parhelion appears as a bright spot on the halo to the right or left of the sun.

For higher sun angles (Fig. 22.34b), ice-crystal geometry causes the sun dogs to move horizontally further away from the sun. For example, at a solar elevation angle of $\Psi = 47°$, the sun dogs are at a horizontal viewing angle of 31° from the sun; namely, they are found outside the 22° halo. As the solar elevation angle becomes greater than about 60°, the sun dog is so faint and so far from the 22° halo that it effectively ceases to exist.

For a single ray input from the sun, let β be the rotation angle of the ice-crystal plate about its column axis. The ray equation for a sun dog is:

(22.18)

$$\theta_V = S_\alpha[S_\alpha(\psi,\beta,\mu_{ai}),\ \ 60° - S_\beta(\psi,\beta,\mu_{ai}),\ \ \mu_{ia}] - \psi$$

$$\theta_H = S_\beta[S_\alpha(\psi,\beta,\mu_{ai}),\ \ 60° - S_\beta(\psi,\beta,\mu_{ai}),\ \ \mu_{ia}] + \beta - 60°$$

where θ_V is the viewing angle of the output ray (elevation above the sun), and θ_H is the viewing angle (azimuth to the right of the sun).

The sun dog as viewed by an observer is the superposition of rays from many ice crystals having a variety of rotation angles. For randomly rotated crystals, there is an equal chance of any β between 0° and 90°. This is simulated on a spreadsheet by solving the sun-dog equation for a large number of equally-spaced β angles. The results are plotted in Fig. 22.35. For a finite-sized ice crystal with aspect ratio typical of hexagonal plates, ray paths with large vertical viewing angle are not physically possible because the light ray would exit or reflect from a basal face before reaching the required prism face.

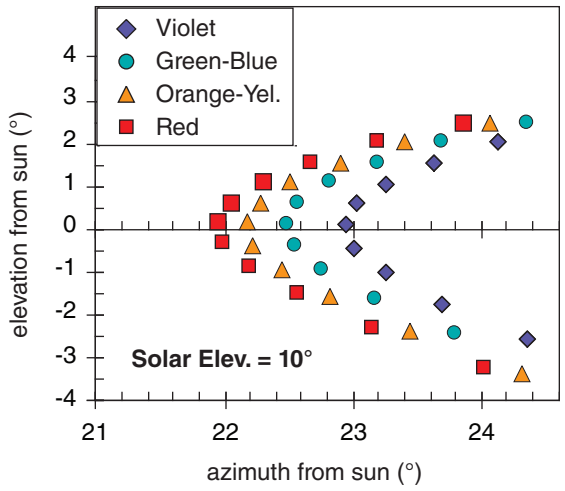

Figure 22.36
Dispersion of colors in a sun dog.

Sun dog colors are similar to the halo, with bright red on the inside (closest to the sun), then orange and yellow, but with green, blue, and violet fading to white (Fig. 22.36 is an expanded view of Fig. 22.35.)

22.3.9. Subsun Dogs (Subparhelia)

Subparhelia (spots of light to the left and right of the subsun) are sketched in Fig. 22.16. Ray geometry for a subsun dog is identical to that for a sun dog, except that the ray within the ice reflects from the inside of the bottom (basal) face (face 2 in Fig. 22.34c), in addition to refractions through prism faces when entering and exiting the crystal.

22.3.10. Tangent Arcs

Tangent arcs are caused when light rays are refracted through large hexagonal column ice crystals, which often fall with their column axis nearly horizontal (Fig. 22.17a). Three phenomena in this tangent-arc category include the **upper tangent arc**, the **lower tangent arc**, and the **circumscribed halo**. We will examine the optics of upper tangent arcs in detail, and then briefly discuss the others.

22.3.10.1. Upper tangent Arc

In Fig. 22.16, the upper tangent arc is just above (and is tangent to) the 22° halo. The shape of this arc changes with solar elevation angle, Ψ.

In the absence of wind shear, the ice-crystal column axes can point in any compass direction within the horizontal plane. Thus, the crystal axis can have any directional orientation γ with respect to the compass direction of the incoming sun ray. The crystal can also have any rotation angle α_1 about the column axis (see Fig. 22.37).

Sample Application

Find the vertical and horizontal viewing angles of a sun-dog ray of red light for solar elevation 40° and crystal rotation $\beta = 45°$.

Find the Answer

Given: $\Psi = 40°$, $\beta = 45°$

Assume for red light: $n_{air} \approx 1.0002753$, $n_{ice} \approx 1.307$

Find: $\theta_V = ?°$, $\theta_H = ?°$

Use eq. (22.18), with $\mu_{ai} = 0.7653$ from before:

$$\theta_V = S_\alpha[S_\alpha(40°, 45°, 0.7653), 60° - S_\beta(40°, 45°, 0.7653), \; 1.3067] - 40°$$

$$\theta_H = S_\beta[S_\alpha(40°, 45°, 0.7653), \{60° - S_\beta(40°, 45°, 0.7653)\}, \; 1.3067] + 45° - 60°$$

For the S_α and S_β inside the square brackets:

$b_{\alpha\beta} = 0.3433$, $S_\alpha = 26.18°$, $S_\beta = 30.37°$

For outside the square brackets: $b_{\alpha\beta} = 2.8448$, because

$S_\alpha[26.18°, (60°–30.37°), 1.3067] =$

$S_\alpha[26.18°, 29.63°, 1.3067] = 39.67°$

$S_\beta[26.18°, 29.63°, 1.3067] = 43.81°$

Finally:

$\theta_V = 39.67° - 40° = \underline{\mathbf{-0.332°}}$

$\theta_H = 43.81° - 15° = \underline{\mathbf{28.81°}}$

Check: Units OK. Physics OK.

Exposition: This portion of the sun dog is nearly at the same elevation as the sun, but is 28.81° to the side of the sun. This is 6.81° outside of the 22° halo.

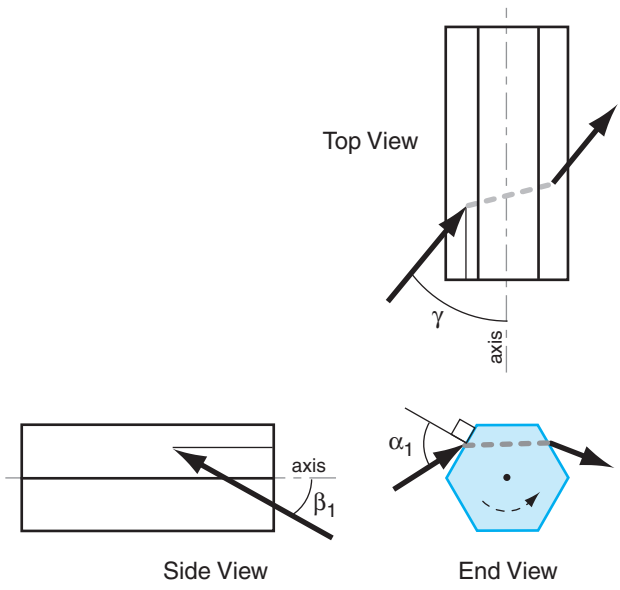

Figure 22.37
Ice crystal geometry associated with upper tangent arcs.

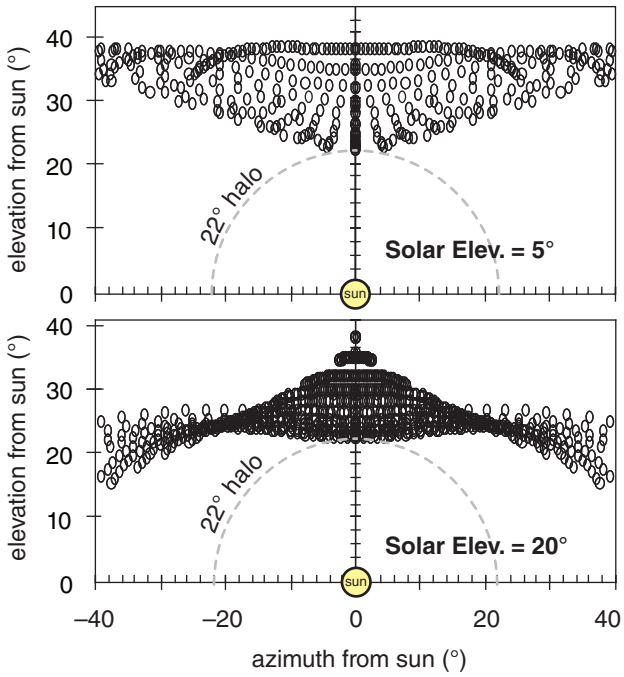

Figure 22.38
The locus of data points (from the solution of eqs. 22.19) shows the upper tangent arc for low solar elevation angles. Regions of sparse data points (corresponding to fainter illumination) have been removed for clarity.

Sample Application

Find the vertical and horizontal viewing angles of a ray of red light in an upper tangent arc for solar elevation $\Psi = 10°$, crystal rotation $\alpha_1 = 76°$, and crystal axis direction $\gamma = 45°$.

Find the Answer

Given: $\Psi = 10°$, $\alpha_1 = 76°$, $\gamma = 45°$.
Assume: $n_{air} \approx 1.0002753$, $n_{ice} \approx 1.307$
Find: $\theta_V = ?°$, $\theta_H = ?°$

Use eqs. (22.19). Various intermediate results are:
$\beta_1 = 76°$
$b_{\alpha\beta} = 0.0402$ (1st calculation)
$\alpha_3 = 21.2°$, $\beta_3 = 38.8°$
$b_{\alpha\beta} = 3.9142$ (2nd calculation)
$\alpha_5 = 22.50°$, $\beta_5 = 57.84°$
$G = 2.701$, $\varepsilon = 75.4°$, $\phi = -30.4°$

Finally:
θ_V = **25.20°**
θ_H = **39.25°**

Check: Units OK. Physics OK.
Exposition: This one data point within the upper tangent arc is above the sun and above the top of the 22° halo, but is off to the right. These calculations would need to be repeated for many other values of input angles to create an image similar to Fig. 22.38

Because there are three input angles for this case, the solution of ray paths is quite nasty. The equations below show how one can calculate the ray output vertical viewing angle θ_V (elevation above the sun), and the horizontal viewing angle θ_H (azimuth from the sun), for any input ray. All other variables below show intermediate steps.

As before, one must examine rays entering many crystals having many angles in order to generate the locus of points that is the upper tangent arc. Even on a spreadsheet, this solution is tedious. For simplicity, no consideration was made for the finite size of the crystal, or for rays that cannot enter the crystal due to reflection, or for rays that are trapped inside because of critical-angle effects.

Given: Ψ, α_1, and γ:

$$\beta_1 = \arctan\left[\cos(\gamma)\cdot\tan(90° - \psi)\right] \qquad (22.19)$$

$$\alpha_3 = 60° - S_\alpha(\alpha_1, \beta_1, \mu_{ai})$$

$$\beta_3 = S_\beta(\alpha_1, \beta_1, \mu_{ai})$$

$$\alpha_5 = 60° - S_\alpha(\alpha_3, \beta_3, \mu_{ia}) - \alpha_1 + \arctan\left[\sin(\gamma)\cdot\tan(90° - \psi)\right]$$

$$\beta_5 = S_\beta(\alpha_3, \beta_3, \mu_{ia})$$

$$G = [\tan(\alpha_5)]^2 + [\tan(\beta_5)]^2$$

$$\varepsilon = \arctan\left[\frac{\tan(\beta_5)}{\tan(\alpha_5)}\right]$$

$$\phi = 90° - \gamma - \varepsilon$$

$$\theta_V = 90° - \psi - \arctan\left[G^{1/2}\cdot\cos(\phi)\right]$$

$$\theta_H = \arctan\left[\sin(\phi)\cdot\left(\frac{G}{1 + G\cdot[\cos(\phi)]^2}\right)^{1/2}\right]$$

To keep the spreadsheet calculations to a finite size, we used γ in the range of 55° to 90°, and α_1 in the range of 0° to 90°. The results for two solar elevations are shown in Fig. 22.38.

The locus of points of the upper tangent arc looks like the wings of a bird. For low solar elevations, the wings are up in the air. As the sun rises in the sky, the wings gently lower. At solar elevations of about 45° or more the wings are wrapped closely around the 22° halo. Above about 60° solar elevation, there is no solution to the upper tangent arc that is physically realistic.

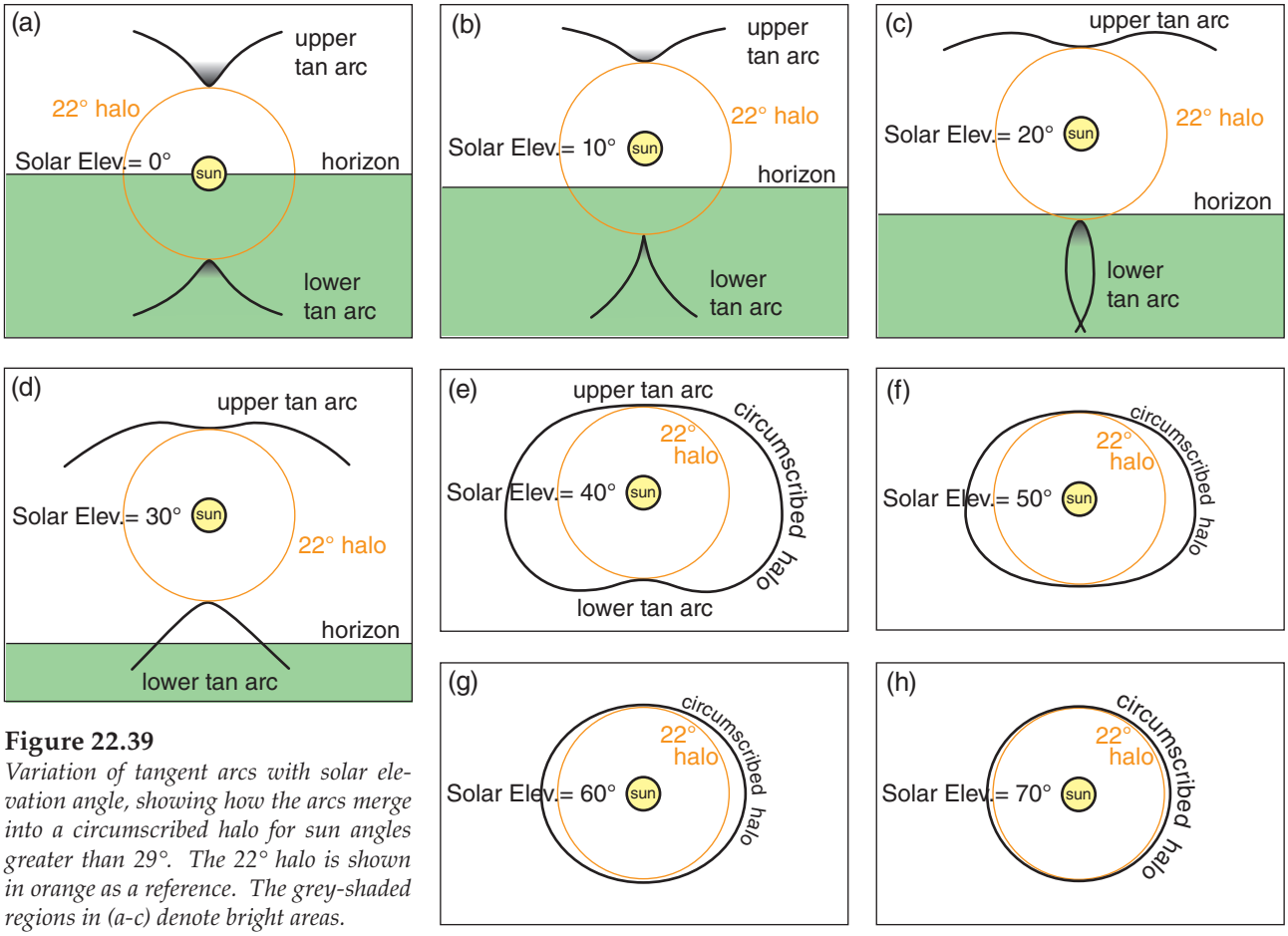

Figure 22.39
Variation of tangent arcs with solar elevation angle, showing how the arcs merge into a circumscribed halo for sun angles greater than 29°. The 22° halo is shown in orange as a reference. The grey-shaded regions in (a-c) denote bright areas.

22.3.10.2. Lower Tangent Arcs

Figs. 22.39 show lower tangent arcs, which occur during the same conditions as upper tangent arcs. Lower tangent arcs are tangent to the bottom of the 22° halo. Upper and lower tangent arcs have similar ray paths (Fig. 22.40) through large hexagonal column ice crystals. Eqs. (22.19) also apply to lower tangent arcs.

For solar elevations of 22° or less, you cannot see the lower tangent arc unless you look down into ice-crystal filled air. You can have such a view from aircraft, mountain peaks, bridges or tall buildings.

22.3.10.3. Circumscribed Halo

At solar elevations of 29° and greater, the upper and lower tangent arcs merge to form a circumscribed halo (Figs. 22.39). At solar elevations above 70°, the circumscribed halo is so tight around the 22° halo that they are often indistinguishable.

22.3.11. Other Halos

Fig. 22.41 and Table 22-3 show most of the halos and arcs.

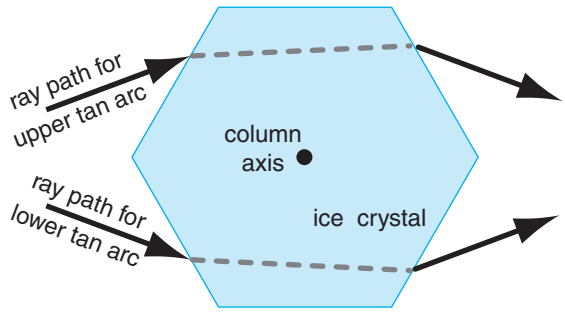

Figure 22.40
Ray paths for upper and lower tangent arcs. This is an end view of a hexagonal column ice crystal that is oriented with a horizontal column axis (out of the page).

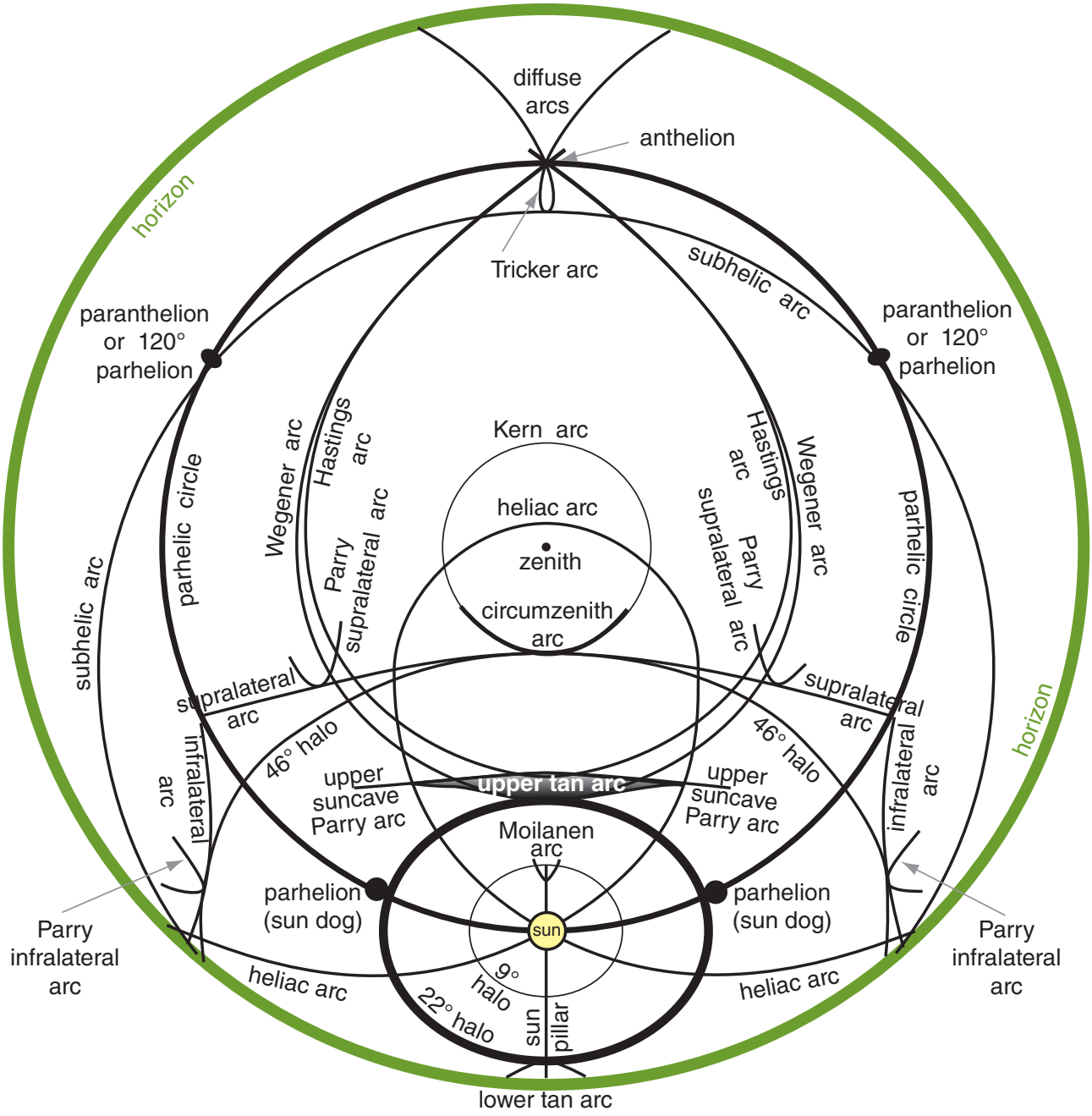

Figure 22.41
Halos in the sky, for a solar elevation of 26°. This view is looking straight up toward the zenith, as what could be photographed using an all-sky camera (with a fish-eye lens). The outermost thick green circle represents the horizon, and the zenith point is marked as a dot in the center of this circle. Some of these halos are extremely rare. Most would not be seen at the same time, because they require ice crystals of different shapes and having perfect orientation. This fish-eye view distorts the 9°, 22°, and 46° halos, which would appear as circles to the observer. The halos of other diameters (including the 28° Scheiner's halo) are not plotted. [Based on data from Les Cowley's website (viewed Jan 2010) http://www.atoptics.co.uk/ , and from W. Tape, 1994: "Atmospheric Halos", and W. Tape and J. Moilanen, 2006: "Atmospheric Halos and the Search for Angle x", published by AGU.]

Table 22-3. Alphabetical catalog of halos. Fig. 22.41 shows most of these halos.

Legend:

Ice crystals:
- A = large oriented hexagonal pyramid
- a = small hex. pyramid (random orientations)
- C = large hexagonal column (col. axis horiz.)
- c = small hex. column (random orientations)
- L = Lowitz large hex. plate (see INFO Box)
- P = large hexagonal plate (col. axis vertical)

Angles:
- 22° ≈ angle of phenomenon from sun, associated with 60° ice wedge angle
- 46° ≈ angle of phenomenon from sun, associated with 90° ice wedge angle

Optics:
- m = (mirror) = one or more reflections
- r = one or more refractions

9° halo, a, r
9° Parry arc, A, r
18° halo, a, r
20° halo, a, r
22° halo, c, r
22° Lowitz arcs (upper & lower), L, r (rare)
22° Parry arcs (upper & lower; suncave & sunvex), C, r
23° halo, a, r
24° halo, a, r
35° halo, a, r
44° parhelia (sun dogs of sun dogs, formed when light passes through 2 hex. plates), 2P, 22°, r
46° halo, c, r
46° Lowitz arcs, L, r (extremely rare)
46° Parry arcs (infralateral, supralateral), C, r
120° parhelia (left & right), P, r, m
Anthelic arc, C, r, m (= Antisolar arc)
Anthelion (a crossing point of diffuse & anthelic arcs)
Antisolar arc, C, r, m (= Anthelic arc)
Circumhorizonal arc, P, 46°, r (also Parry)
Circumscribed halo, C, 22°, r
Circumzenithal arc, P, 46°, r (also Parry)
Diffuse arcs, C, r, m
Halos (see 9° through 46° halos above)
Hastings arcs (of upper suncave Perry arc; and of lower suncave Perry arc), r, m
Heliac arc, C, m or (r, m)
Infralateral arc, C, 46°, r (also Parry)
Kern arc, P, 46°, r, m (rare)
Lower suncave Parry arc, C, 22°, r
Lower sunvex Parry arc, C, 22°, r
Lower tangent arc, C, 22°, r
Lower Wegener arc, C, r, m
Lowitz arcs (upper & lower), L, 22°, r (rare)
Moilanen arc (rare; seen in ice crystals from snow-making machines)
Paranthelia (= 120° parhelia, left & right), P, r, m
Parhelia (sun dogs) (left & right), P, 22°, r
Parhelic circle, [P, m or (r, m)] or [C, m or (r, m)] (also Parry)
Parry arcs (Many arcs. See separate listings for: 9°, upper suncave, upper sunvex, lower suncave, lower sunvex, circumzenithal, circumhorizonal, infralateral, supralateral, Hastings, helic, subhelic, anthelic, subanthelic) (see Fig. 22.41)
Scheiner's 28° halo (from cubic Ic ice crystals), r
Subanthelic arc, C, r, m
Subcircumzenith arc, P, 46°, r, m (not yet observed)
Subhelic arc, C, r, m
Subhorizon halo (halos and arcs below the horizon, including portions of diffuse, Tricker, subhelic, lower Wegener, and lower tangent arcs)
Subparhelia (subsun dogs) (left & right), P, 22°, r, m
Subparhelic circle, [P, r, m] or [C, r, m]
Subsun, P, r
Subsun dogs (subparhelia) (left & right), P, 22°, r, m
Sun dogs (parhelia) (left & right), P, 22°, r
Sun pillar, C or P, r
Supralateral arc, C, 46°, r (also Parry)
Tangent arc (upper & lower), C, 22°, r
Tricker arc, C, r, m
Upper suncave Parry arc, C, 22°, r
Upper sunvex Parry arc, C, 22°, r
Upper tangent arc, C, 22°, r
Upper Wegener arc, C, r, m
Wegener arcs (upper & lower), C, r, m

INFO • Special Crystal Orientations

A **Parry-oriented column** crystal has both a horizontal column axis and horizontal top and bottom prism faces (see Fig. at right). Resulting **Parry arcs** (Fig. 22.41) are observed 1% as frequently as 22° halos.

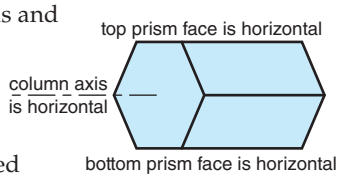

Fig. 22.b

A **Lowitz-oriented plate** crystal has an unusual orientation. **Lowitz arcs** are extremely rare & faint (not shown in Fig. 22.41).

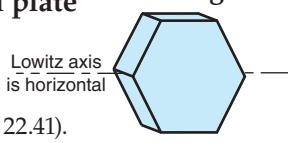

Fig. 22.c

INFO • Scheiner's Halo

In year 1629, Christopher Scheiner observed a rare 28° halo. It has been observed only about 6 times since then. One explanation is that sun rays pass through an octahedral crystal made of cubic ice (Ic). Cubic ice is discussed in an INFO Box in the Precipitation chapter. The Fig. below shows a ray path through a truncated octahedron.

The wedge angle of 70.528° yields a minimum viewing angle of 27.46° according to eq. (22.16), assuming a refractive index of 1.307. This cubic-ice explanation is still being debated.

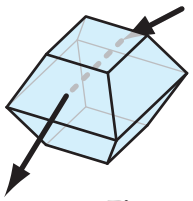

Fig. 22.d

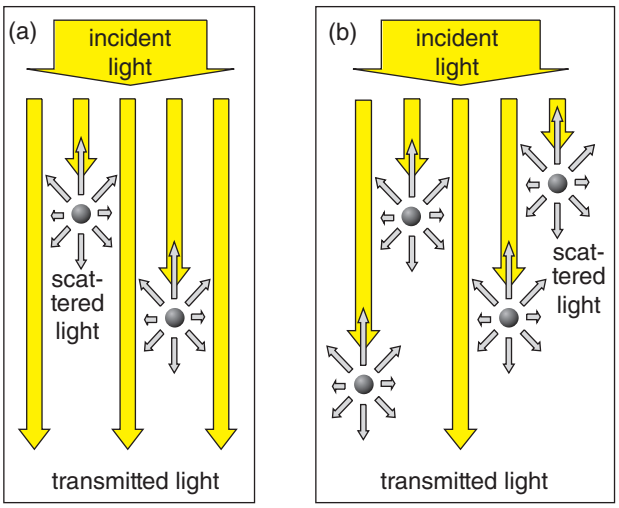

Figure 22.42
Incident light (long downward arrows) can be scattered (small arrows in all directions) by particles (grey dots) that are in the path of the light. Paths with few particles (a) scatter less light and transmit more light than paths with many particles (b).

Sample Application
What fraction of light is scattered for $\tau = 2$?

Find the Answer
Given: $\tau = 2$
Find: $I_{scat}/I_o = ?$

Use eq. (22.21): $I_{scat}/I_o = 1 - e^{-2} = 0.865$ = **86.5%**

Check: Units OK. Magnitudes agree with text.
Exposition: A large portion of light is scattered. This optical depth can occur in polluted air.

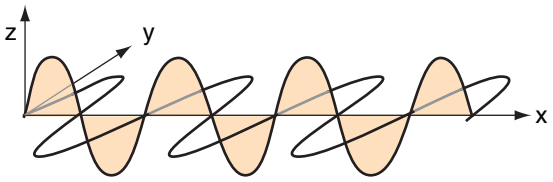

Figure 22.43
Unpolarized light consists of two cross-polarized parts.

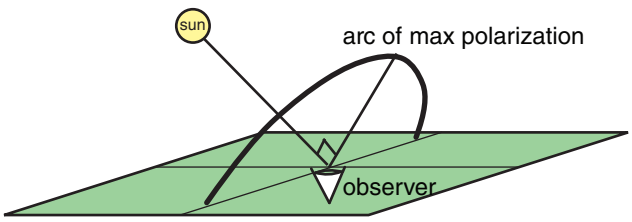

Figure 22.44
Arc of max polarization in the sky due to Rayleigh scattering.

22.4. SCATTERING

22.4.1. Background

22.4.1.1. Optical thickness

Light can scatter off of air molecules, pollutant particles, dust, and cloud droplets. More particles in the air cause more of the light to be scattered (Fig. 22.42). The ratio of transmitted (I_{tran} , non-scattered) to incident (I_o) light can be quantified using the **optical thickness** or **optical depth** τ (dimensionless) in Beer's Law:

$$\frac{I_{tran}}{I_o} = e^{-\tau} \qquad (22.20)$$

Thus, the relative amount of light scattered (I_{scat}) is:

$$\frac{I_{scat}}{I_o} = 1 - \frac{I_{tran}}{I_o} = 1 - e^{-\tau} \qquad (22.21)$$

Zero optical thickness means no light is scattered, while $\tau > 5$ implies that virtually all the light is scattered. Optical thickness increases for longer paths and for higher particle concentrations. Examples are $\tau = 0.03$ to 0.3 for a clean dry atmosphere, and $\tau > 10$ for thick clouds.

22.4.1.2. Polarization

Light propagating in the *x*-direction can be thought of as having oscillations in the *y* and *z* directions (Fig. 22.43). This is unpolarized light. Polarizing filters eliminate the oscillations in one direction (for example, the shaded curve) while allowing the other oscillations to pass through. What remains is **polarized** light, which has half the intensity of the unpolarized ray.

Sunlight becomes polarized when it is scattered from air molecules. The maximum amount of polarization occurs along an arc in the sky that is 90° from the sun, as viewed from the ground (Fig. 22.44).

If the sky scatters light with one polarity, and a polarizing camera filter or polarized sunglasses are rotated to eliminate it, then virtually no sky light reaches the camera or observer. This makes the sky look very deep blue, providing a very striking background in photographs of clouds or other objects. If you want to maximize this effect, pick a camera angle looking toward the 90° arc from the sun.

22.4.1.3. Types of Scattering

The type and efficiency of scattering depends on the ratio of particle diameter *D* to the wavelength λ of the light. Table 22-4 summarizes the types of scattering. Actual size ranges of cloud droplets and aerosols are wider than indicated in this table.

Table 22-4. Scattering of visible light. D = particle diameter. λ = wavelength of light.					Scattering Varies with		
D / λ	**Particles**	**Diameter, D (μm)**	**Type**	**Phenomena**	**λ**	**Direction**	**Polarization**
< 1	air molecules	0.0001 to 0.001	Rayleigh	blue sky, red sunsets	X		X
≈ 1	aerosols (smog)	0.01 to 1.0	Mie	brown smog	X	X	X
> 1	cloud droplets	10 to 100	geometric	white clouds		X	

22.4.2. Rayleigh Scattering

Air molecules have sizes of $D \approx 0.0001$ to 0.001 μm, which are much smaller than the wavelength of light (λ = 0.4 to 0.7 μm). These particles cause **Rayleigh scattering**. The ratio of scattered intensity of radiation I_{scat} to the incident radiation intensity I_o is:

$$\frac{I_{scat}}{I_o} \approx 1 - \exp\left[-\frac{a\cdot(n_{air}-1)^2}{\rho\cdot\lambda^4}\cdot x\right] \qquad (22.22)$$

where a = $1.59\text{x}10^{-23}$ kg, ρ is air density, n_{air} is the refractive index, and x is the path length of light through the air.

Fig. 22.45a shows the relative amount of scattering vs. wavelength. Because of the λ^{-4} dependence, shorter wavelengths such as blue and violet are scattered much more (about a factor of 10) than red light, which causes our **blue sky** color. For light shining vertically through a clean dry atmosphere, $\tau = 0.3$ for violet light and 0.03 for red.

Sunlight intensity varies according to Planck's law (Fig. 22.45b and the Solar & Infrared Radiation chapter). The product of the top 2 curves shows the amount of sunlight that is scattered in the atmosphere (Fig. 22.45c). All curves have been normalized to have a maximum of 1.0.

The curve in Fig. 22.45c peaks in the ultraviolet portion of the spectrum. Although this is not visible to the naked eye, the scattered ultraviolet light can affect photographic films to produce a picture that looks hazier than the view by eye. Haze filters on cameras can filter out this unwanted scattered ultraviolet light.

22.4.3. Geometric Scattering

For large particles such as cloud droplets, light is reflected according to geometric optics. Because all wavelengths are reflected equally, **clouds look white** when illuminated by white sunlight.

There is, however, a directional dependence. Light that is scattered in the same direction that the incident ray is pointing is called **forward scattering**. The opposite is **backward scattering**. For clouds, forward scattering is usually greater than backscattering. Thus, clouds you see in the direction of the sun look bright white, while those in the direction of your shadow look slightly more grey.

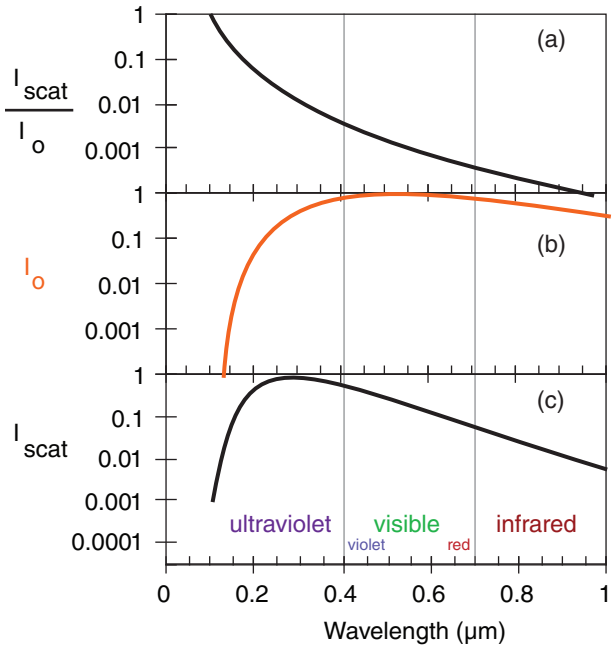

Figure 22.45
Top: Relative Rayleigh scattering. Middle: Planck spectrum for the sun. Bottom: product of the top two curves, indicating the amount of sunlight scattered in clean air.

Sample Application

What fraction of incident violet light is scattered by air molecules along a 20 km horizontal ray path near the Earth?

Find the Answer

Given: $x = 5\text{x}10^6$ m, $\lambda = 4\text{x}10^{-7}$ m for violet
Find: I_{scat}/I_o = ?
Assume: $\rho = 1$ kg·m^{-3} for simplicity.

Use eq. (22.22): $I_{scat}/I_o =$

$$1 - \exp\left[-\frac{(1.59\times10^{-23}\,\text{kg})\cdot(0.0002817)^2}{(1\ \text{kg}\cdot\text{m}^{-3})\cdot(4\times10^{-7}\,\text{m})^4}\cdot(2\times10^4\,\text{m})\right]$$

$= \underline{\mathbf{0.627}}$ = 62.7% scattered

Check: Units OK. Physics OK.
Exposition: Looking toward the horizon, distant objects are difficult to see because some of the light is lost. Vertical rays experience less scattering, because air density decreases with height.

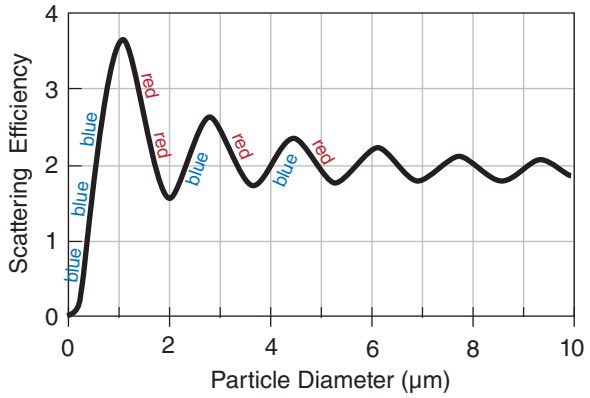

Figure 22.46
Mie scattering efficiency and dominant color scattered out of white light for various particle diameters.

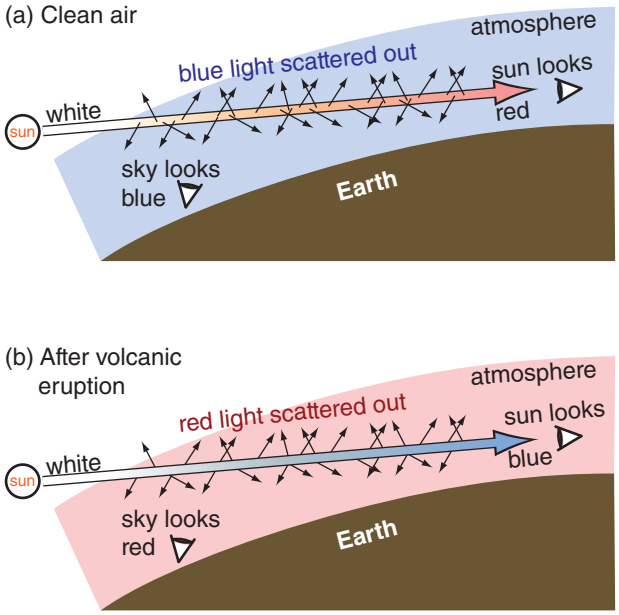

Figure 22.47
Scattering of sunlight as it travels through a long path through the atmosphere. (a) Clear skies. (b) Air hazy due to tiny sulfuric-acid aerosol droplets suspended in the stratosphere after a volcanic eruption.

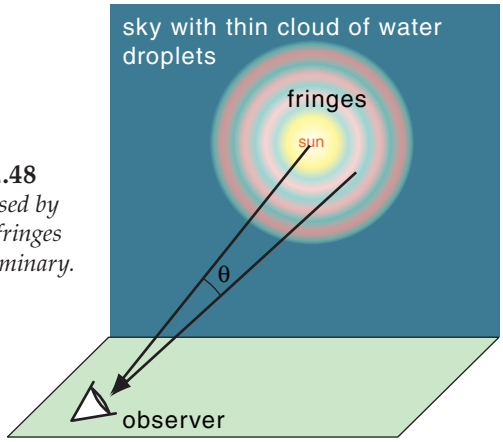

Figure 22.48
Corona caused by diffraction fringes around a luminary.

22.4.4. Mie Scattering

Gustov Mie proposed a comprehensive theory that describes reflection, scattering, polarization, absorption, and other processes for particles of all sizes. The theory reduces to Rayleigh scattering for particles smaller than the wavelength of light, and to geometric scattering for larger particles. Aerosol particles have an intermediate size, so no simplification of Mie theory is possible.

Fig. 22.46 shows that aerosols with diameters greater than about 0.1 μm are 10 to 1000 times more efficient light scatterers than air molecules, which is why polluted air looks hazy and has low visibility. Uniform aerosol smog particles can produce bluish or reddish-brown colors, depending on the dominant aerosol diameter.

Most aerosol particles have diameters smaller than 1 μm. Fig. 22.46 shows that these aerosols still scatter more blue light than red, causing blue haze. When the sun is low in the sky, the light rays travel through a very long path of air en route to the observer. For this situation, so much blue light is scattered out (making our **blue sky**) by these small aerosols and air molecules that it leaves more red in the remaining direct beam — giving a beautiful **red sun** at sunrise or sunset (Fig. 22.47a).

However, some acid droplet aerosols have diameters of about 1.5 μm, which scatters more red than blue. In some polluted regions where combustion processes emit SO_2 and NO_2 into the air, these pollutants can react with water in the air to form sulfuric acid and nitric acid. Scattering in this condition creates a **brown cloud** haze.

Another source of 1.5 μm diameter acid aerosols is volcanic eruptions, where sulfur emissions change into sulfuric acid droplets in the stratosphere. When the sun is low in the sky, so much red light is scattered out that beautiful **crimson sunset skies** are often observed after volcanic eruptions (Fig. 22.47b). Also, this leaves the remaining direct beam of sunlight in the setting sun slightly blue, which is hard to see because it is so bright. However, direct moonlight from a rising or setting moon can often be blue — causing a **blue moon** after a volcanic eruption.

For aerosols, forward scattering is usually greater than backscattering. Scattering can be polarized.

22.5. DIFFRACTION & INTERFERENCE

When sunlight or moonlight passes through a thin cloud of water droplets, diffraction and interference can produce a disk of bright sky centered on the luminary (light source), surrounded by one or more colored rings or **fringes** (Fig. 22.48).

Recall from physics that when wave fronts hit the edge of an object, part of the wave bends around the edge — a process called **diffraction**. This is consistent with Huygens' principle, where every point on an incident wave front can be thought of as a source of new wavelets radiating away, and where the subsequent position of the wave front depends on the superposition of the wavelets. An analogy is ocean waves moving past vertical posts or pilings.

Fig. 22.49a sketches cloud droplets and the wave fronts of incident light from the sun or moon. The edge of each droplet is marked with an "x". Consider the wavelets generated from each edge, sketched as the thin grey concentric circles. Superposition of these wavelets, indicated with the thick tan wavy line, can **constructively interfere** to create a new wave train. Fig. 22.49a shows one of the resulting wave trains — the one for light that is transmitted straight through the cloud to the observer. Other angles have **destructive interference**.

However, there are many other angles where the wavelet fronts constructively interfere, one of which is sketched in Fig. 22.49b. This has the net effect of producing an additional train of wave fronts that leaves the cloud at a different angle. Because this angle of light leaving the cloud is the same as the angle observed by the observer, the observer sees the constructive interference (i.e., bright light) from all those different drops that happen to be the same viewing angle away from the sun. The different angles that can be produced from a set of drops produces many rings of different radii, called fringes.

The angle θ to each ring depends on the radius R of the droplet and the wavelength λ of light:

$$\theta = \arcsin\left(\frac{m \cdot \lambda}{R}\right) \qquad (22.23)$$

where m is a dimensionless diffraction parameter given in Table 22-5.

For any one color, there are faint rings of light separated by darker gray background. The different colors of the spectrum have different fringe radii, causing the fringes of any one color (e.g. blue-green) to appear in the dark spaces between fringes of another color (e.g., red). Fringes further from the sun (with higher fringe index) are less bright, as given in Table 22-5 and plotted in Fig. 22.50.

22.5.1. Corona, Iridescence and Glory

Wave clouds (standing **lenticular** clouds) have extremely uniform drop sizes. This means that all the drops in the cloud produce the same fringe angles, for any one color. Hence, the diffraction from all the droplets reinforce each other to produce bright colorful fringes (rings) called **corona**. Most

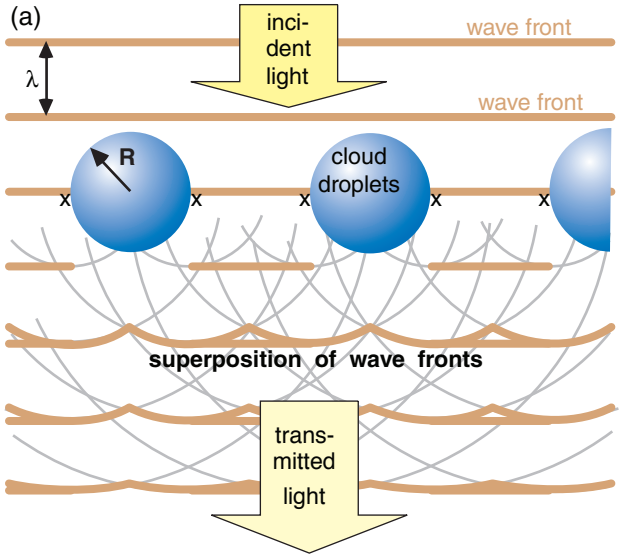

Figure 22.49a
Diffraction of light from edges of cloud droplets.

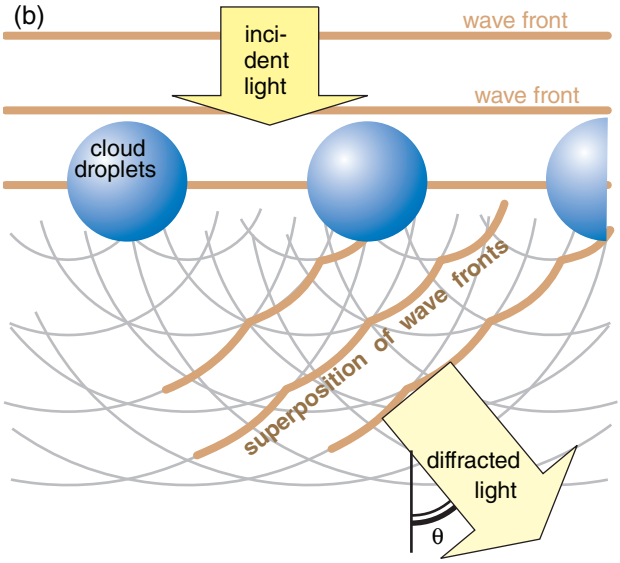

Figure 22.49b
Another direction where constructive interference happens.

Table 22-5. Diffraction fringes.

Fringe Index	m	Relative Intensity
1	0	1.0
2	0.819	0.01745
3	1.346	0.00415
4	1.858	0.00165
5	2.362	0.00078
6	2.862	0.00043
7	3.362	0.00027
8	3.862	0.00018

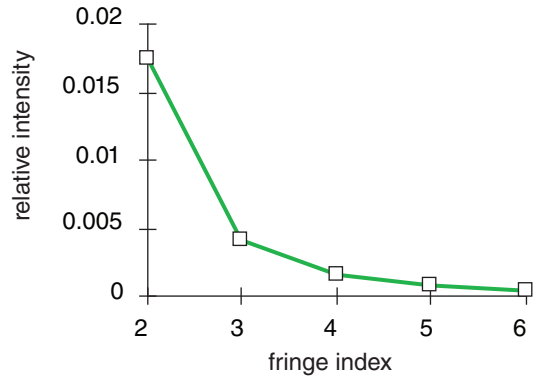

Figure 22.50
Diffraction fringe brightness. Larger indices indicate fringes that are further from the luminary.

Sample Application

The first visible fringe (index = 2) of red is 10° from the moon. What is the cloud drop radius?

Find the Answer

Given: $\theta = 10°$, $\lambda = 0.7$ μm.
$m = 0.819$ from Table 19-3 for fringe #2.
Find: $R = ?$ μm
Assume $n_{air} \approx 1.0002753$ for red light.

Rearrange eq. (22.23):

$$R = \frac{m \cdot \lambda}{\sin\theta} = \frac{0.819 \cdot (0.7\mu m)}{\sin(10°)} = \underline{\mathbf{3.3\ \mu m}}$$

Check: Units OK. Physics OK.
Agrees with Fig. 22.51.
Exposition: Smaller than typical cloud-droplet size, perhaps associated with a wave cloud.

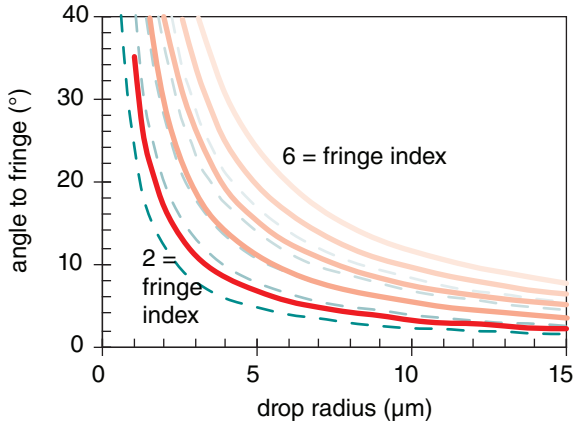

Figure 22.51
Viewing angle vs. cloud droplet size, for red (solid) and blue-green (dashed) diffraction fringes.

other clouds contain drops with a wide range of sizes, causing the colors to smear together to form a whitish disk (called an **aureole**) touching the sun or moon.

Eq. (22.23) can be solved on a spreadsheet for various cloud droplet sizes and colors. The results in Fig. 22.51 show that smaller droplets produce larger-diameter fringes. For reference, typical cloud droplets have 10 μm radii, and the viewing angle subtended by the sun is 0.534°.

To help discriminate between corona and halos, remember that corona are bright disks of light that touch the sun or moon, while halos have a dark region between the luminary and the halo ring. Also, corona are formed from liquid water droplets, while halos are formed from ice crystals.

Droplets near the edges of clouds (particularly wave clouds) can be very small as they form or evaporate, and can cause fringes of very large angular radius. As a result, the edges of clouds near the sun or moon are often colorful, a phenomenon called **iridescence**.

When looking down from above a cloud, diffraction patterns are sometimes seen around the shadow of the observer. This is called **glory**, and is associated with both diffraction and reflection from the cloud droplets. When viewed from an aircraft flying above the clouds, the glory is a circle of light centered on the shadow of the airplane.

22.5.2. Supernumerary Bows

As sketched in Fig. 22.7, supernumerary bows are closely spaced faint pinkish-purple and turquoise diffraction arcs touching the inside of the primary rainbow arc. The viewing-angle width of this bow (containing 2 to 4 sequences of fringes) is 1 to 2°. Supernumerary bows are most visible when the raindrop diameter is smaller than about 1 mm, during a rain shower when most of the falling drops have nearly the same size (i.e., a narrow drop-size distribution).

When the rain shower has a wider drop-size distribution, the greater flattening of the larger drops causes many drops to have nearly the same vertical thickness, even though their horizontal diameters vary widely. Thus, supernumerary bows are often most visible inside the top of the rainbow arc (because drops of equal vertical thickness cause equal diffraction fringes that constructively interfere), and less visible inside the sides. Rainbows and supernumerary bows are also visible when the sun shines on dew drops on grass, and in water sprays from irrigation systems. Very faint supernumerary bows can sometimes be seen outside the secondary rainbow.

To explain the optics, look at Fig. 22.13b and consider red light at viewing angle 40°, for example. We

see that light at this viewing angle comes from two different paths through the raindrop: one at impact parameter 0.74 and the other at impact parameter 0.94. These two different paths travel different distances through the drop, hence their wave fronts can get out of phase with each other. At certain angles for certain colors the wave fronts interfere with each other, canceling to yield no light of that color. At other angles for other colors, the wave fronts are in phase and reinforce each other, yielding a bright color. This **constructive and destructive interference** of wave fronts creates supernumeraries.

22.6. MIRAGES

Refractive index n_{air} varies with air density ρ:

$$n_{air} - 1 \approx (n_{ref} - 1) \cdot \rho / \rho_{ref} \qquad (22.24)$$

where *ref* denotes a reference condition (such as given for air at any of the T and P values in Table 22-1). Knowing T and P, you can use the ideal gas law to find density [$\rho = P/(\Re \cdot T)$ for $\Re = 0.287$ (kPa K^{-1})·(m^3 kg^{-1}); see Chapter 1 for details]. Thus, you can rewrite eq. (22.24) as:

$$n_{air} - 1 = (n_{ref} - 1) \cdot \frac{T_{ref}}{T} \cdot \frac{P}{P_{ref}} \qquad (22.25)$$

A sharp change in density between two media causes a sharp kink in the ray path (Fig. 22.1). A gradual change of density causes a smoothly curving ray path (Fig. 22.52). The radius of curvature R_c (positive for concave up) is:

$$R_c \approx \frac{\rho_{ref}}{(n_{ref} - 1) \cdot (\cos\alpha) \cdot (\Delta\rho / \Delta z)} \qquad (22.26)$$

where α is the angle of the ray above horizontal, and the gradient of density $\Delta\rho/\Delta z$ is assumed to be perpendicular to the Earth's surface.

Substituting the ideal gas law and the hydrostatic relationship from Chapter 1 into eq. (22.26) yields:

$$R_c \approx \frac{-(T / T_{ref}) \cdot (P_{ref} / P)}{(n_{ref} - 1) \cdot (\cos\alpha) \cdot \left\{ \frac{1}{T} \left[\frac{\Delta T}{\Delta z} + a \right] \right\}} \qquad (22.27)$$

where $a = 0.0342$ K·m^{-1} .

Because average density decreases with height in the atmosphere (see Chapter 1), eq. (22.27) gives a negative radius of curvature in the presence of weak temperature gradients. In other words, the ray is bent downward in a standard atmosphere. This

Sample Application
During winter with cold (T = –30°C) high-pressure (P = 104 kPa), find the refractive index for violet light.

Find the Answer
Given: T = –30°C = 243 K, P = 104 kPa, λ = 0.4 μm.
Find: n_{air} = ? (dimensionless)

Use Table 22-1: For T_{ref} = –20°C = 253K & P_{ref} = 101.325 kPa, the table gives n_{ref} = 1.0003219, assuming RH=75%.

Use eq. (22.25):
$n_{air} = 1 + (0.0003219) \cdot (253/243) \cdot (104/101.325)$
$= \underline{\mathbf{1.0003440}}$

Check: Value reasonable compared to Table 22-1.
Exposition: By the ideal gas law, air density increases when temperature decreases and pressure increases. Higher density gives greater refractive index.

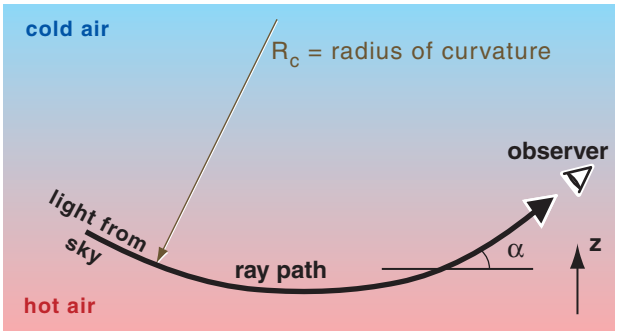

Figure 22.52
Ray curvature within a vertical gradient of density, creating an inferior mirage.

Sample Application
What is the radius of curvature of a horizontal indigo (λ ≈ 0.45 μm from Table 2-3 in the Radiation chapter) ray near the ground in a standard atmosphere?

Find the Answer
Given: z = 0, α = 0°,
n_{air} ≈ 1.00028 from Table 22-1 for indigo light.
Find: R_c = ? km

Assume T = 288K and P = 101.3 kPa in a standard atmosphere near the ground. Assume the vertical temperature gradient is negligible. Rearrange eq. (22.27):

$$R_c \approx \frac{-1}{(0.00028) \cdot (\cos 0°) \cdot (0.0342\text{K} \cdot \text{m}^{-1} / 288\text{K})}$$
$$= \underline{\mathbf{-30{,}000\ km}}$$

Check: Units OK. Physics OK.
Exposition: The large negative radius implies very weak downward curvature, which agrees with the small angle of the **apparent sunrise** (Table 2-2).

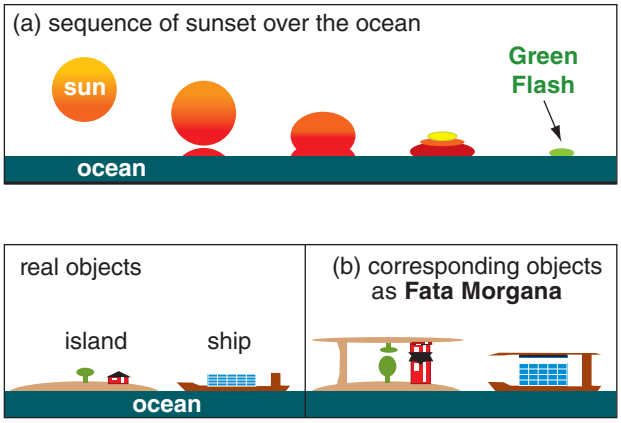

Figure 22.53
(a) Appearance of the sun setting over the ocean in inferior mirage conditions. (b) Distortion of distant objects during Fata Morgana mirage.

INFO • Newton and Colors

To confirm his laws of motion, Isaac Newton wanted to view the motions of the planets. He built his own telescopes for this purpose. However, the images he observed through his lenses were blurry. For example, images of stars were spread (**dispersed**) into a streak of colors.

After experimenting with different lenses, he concluded that neither the glass nor the construction was flawed. He realized that there must be some unknown physics causing this optical phenomenon. Like many great scientists, he allowed himself to get side-tracked to study this phenomenon in detail.

One of his experiments was to obtain a triangular prism, and to allow sunlight to pass through it. He observed that the white sunlight is composed of a spectrum of colors: red, orange, yellow, green, blue, indigo, and violet. Newton must have had a unique sense of color, because most people cannot discriminate between indigo and violet in the spectrum.

Newton concluded that the refraction of light through a lens inevitably causes color **dispersion**. Thus, a pinpoint of white starlight would be spread into a smear of colors. His solution to the telescope problem was to design a telescope without glass lenses. Instead he invented a reflecting telescope using curved mirrors, because reflection does not cause separation of light into colors.

agrees with Huygens' principle, that says light rays are bent toward media of higher density.

For ray paths near horizontal, the total bending through the whole atmosphere is about 0.567°, which is why **apparent sunrise** occurs before geometric sunrise (see the Radiation chapter). In everyday life, we rarely notice refraction associated with the standard atmosphere. However, in the presence of strong temperature gradients we can see mirages.

For rays to bend up instead of down, the term in square brackets in eq. (22.27) must be negative. This is possible when $\Delta T/\Delta z < -a$. A temperature decrease of at least 3.5°C per 10 cm height rise is necessary. Such a strong gradient is possible on hot sunny days in the air touching strongly-absorbing (black) surfaces. This condition of warm air under cold causes **inferior mirages**, where the objects appear lower than they really are. Warm under cold air is statically unstable (see the Atmospheric Stability chapter), causing turbulence that makes these mirages shimmer.

Inferior mirages are common above black roads on hot sunny days. Looking down toward the road, you see light rays refracted from the sky (Fig. 22.52). As these shimmer in the convective turbulence, the mirages look similar to reflections from the surface of water puddles.

Inferior mirages can also form over the ocean, if a thin layer of warm air is created by heat conduction from a warm sea surface, but colder air exists aloft. As the sun sets over the ocean, the base of the sun sometimes appears to spread out (Fig. 22.53a), causing the shape of the sun's outline to look like the Greek letter omega (Ω). Later, just as the top of the sun sets, the inferior-mirage effect causes the top of the sun to briefly appear emerald green just before it disappears below the horizon. This phenomenon is called **green flash**. *[CAUTION: to avoid damaging your eyes, do not look directly at the sun.]*

Cold air under warm air (as during early morning over land, or in arctic regions over ice, or where warm air flows over cold seas) causes **superior mirages**, where objects appear higher than they are. This accentuates the downward bending of rays, causing the image of the object to **loom** or stretch vertically upward.

The **Fata Morgana** mirage is caused by light rays passing through one or more elevated temperature inversions (a sharp interface between cold air below and warmer air aloft). Some ray paths bend as in superior mirages, and others bend as in inferior mirages. This causes portions of normal objects to appear stretched in the vertical, and other portions to appear compressed (Fig. 22.53b) or flipped.

The results are fanciful images of mountains, ramparts, and castle turrets (some of which appear to float above ground) where none exist in reality.

The name of this mirage comes from Fairy Morgan (or Fata Morgana in Italian) of the King Arthur legend, an enchantress/magician who could create illusions of floating castles, etc.

22.7. REVIEW

Atmospheric optical phenomena can be caused by reflection, refraction, scattering, diffraction and interference. Some of these processes are caused by the difference in density between hydrometeors (liquid and solid water particles) and air.

Common ice-crystal optical phenomena include the sun pillar, parhelic circle, subsun, 22° halo, 46° halo, circumzenithal arc, sun dogs, subsun dogs and tangent arcs. They are usually found by looking toward the sun. The hexagonal column shape of many ice crystals creates 60° and 90° prismatic effects. The somewhat random orientation of these crystals causes sunlight to be returned in different directions from different crystals. The phenomena we see are the superposition from many crystals. Many other rarer halos can occur, some of which are associated with hexagonal pyramid crystals.

Raindrop phenomena are a bit easier to describe, because the approximate spherical shape eliminates orientational dependence. Rainbows are seen by looking away from the sun. Cloud droplets produce corona, iridescence, glory, and aureole. Scattering by air molecules cause blue sky and red sunsets. Refraction in air causes amazing mirages.

22.7.1. Postface

This brings you to the end of this book. Along the way, you examined the physics of atmospheric pressure, wind, temperature, and humidity. You saw how these concepts weave together to make the cyclones, precipitation, thunderstorms, fronts, and hurricanes that we experience as weather. You have the quantitative wherewithal to critically evaluate weather-related issues, and to consider sound decisions that affect society and the future of our planet.

If this is your last course on meteorology, be confident that you have the background to delve into the meteorology journals to learn the latest details that might help you in your engineering or scientific work. If you plan to continue your study of meteorology, the overview that you have gained here will help you put into context the advanced material that you will soon be learning.

As a farewell, I invoke an Irish blessing: "May the wind be always at your back, may the sun shine warm upon your face, and may the rains fall soft upon your fields." Sincerely, *Roland Stull*

A SCIENTIFIC PERSPECTIVE • Great Scientists Can Make Big Mistakes Too

Isaac Newton explained many atmospheric optical phenomena in his books on optics. Not all his theories were correct. One of his failures was his explanation of the blue sky.

He thought that the sky was blue for the same reason that soap bubbles or oil slicks have colors. For blue sky, he thought that there is interference between light reflecting from the backs of small water droplets and the light from the front of the drops.

Although Newton's theory was accepted for about 175 years, eventually observations were made of the polarization of sky light that were inconsistent with the theory. Lord Rayleigh proposed the presently accepted theory in 1871.

Like Newton, many great scientists are not afraid to propose radical theories. Although most radical theories prove to be wrong, the few correct theories are often so significant as to eventually create **paradigm shifts** (radical changes) in scientific thought. Unfortunately, "publish or perish" demands on modern scientists discourage such "high risk, high gain" science.

22.8. HOMEWORK EXERCISES

22.8.1. Broaden Knowledge & Comprehension

B1. Search the web for images of the following atmospheric optical phenomena:

a. 22° halo	b. 46° halo
c. sun dogs	d. sub sun dogs
e. sub sun	f. sun pillar
g. supersun	h. upper tangent arc
i. parhelic circle	j. lower tangent arc
k. white clouds	l. circumzenithal arc
m. Parry arcs	n. primary rainbow
o. red sunset	p. secondary rainbow
q. blue sky	r. Alexander's dark band
s. corona	t. crepuscular rays
u. iridescence	v. anti-crepuscular rays
w. glory	x. fata morgana
y. green flash	z. mirages
aa. halos other than 22° and 46°	
ab. circumhorizonal arc	ac. circumscribed halo
ad. Lowitz arcs	ae. Scheiner's halo
af. Moilanen arc	ag. Hastings arc
ah. Wegener arc	ai. supralateral arc

aj. infralateral arcs ak. subhelic arc
am. heliac arc an. diffuse arcs
ao. Tricker arc ap. 120° parhelia (120° sun dogs)
aq. various subhorizon arcs
ar. fog bow as. blue moon
at. reflection rainbow au. twinned rainbow
av. supernumerary bows

B2. Search the web for images and descriptions of additional atmospheric phenomena that are not listed in the previous question.

B3. Search the web for microphotographs of ice crystals for ice Ih. Find images of hexagonal plates, hexagonal columns, and hexagonal pyramids.

B4. Search the web for diagrams or microphotographs of ice crystals for cubic ice Ic.

B5. Search the web for lists of indices of refraction of light through different materials.

B6. Search the web for highway camera or racetrack imagery, showing inferior mirages on the roadway.

B7. Search the web for computer programs to simulate atmospheric optical phenomena. If you can download this software, try running it and experimenting with different conditions to produce different optical displays.

B8. Search the web for images that have exceptionally large numbers of atmospheric optical phenomena present in the same photograph.

B9. Search the web for information on linear vs. circular polarization of sky light. Polarizing filters for cameras can be either circular or linear polarized. The reason for using circular polarization filters is that many automatic cameras loose the ability to auto focus or auto meter light through a linear polarizing filter. Compare how clear sky would look in a photo using circular vs. linear polarization filters.

B10. Search the web for literature, music, art, or historical references to atmospheric optical phenomena, other than the ones already listed in this chapter.

B11. Search the web for info on the history of scientific understanding of atmospheric optical phenomena. (E.g., Snell's law, etc.)

22.8.2. Apply

A1. Calculate the angle of reflection, given the following angles of incidence:

a. 10° b. 20° c. 30° d. 40° e. 45
f. 50° g. 60° h. 70° i. 80° j. 90°

A2. Find the refractive index for the following (medium, color) for T = 0°C and P = 80 kPa.

a. air, red b. air, orange c. air, yellow
d. air, green e. air, blue f. air, violet
g. water, red h. water, orange i. water, yellow
j. water, green k. water, blue
m. ice, red n. ice, orange o. ice, yellow
p. ice, green q. ice, blue r. ice, violet

A3. Find the speed of light for the medium and color of the previous exercise.

A4. Find the ratio μ of refractive indices for the following pairs of medium from exercise A2:

a. (a, g) b. (a, m) c. (g, m) d. (b, h) e. (b, n)
f. (h, n) g. (c, i) h. (c, o) i. (i, o) j. (d, j)
k. (d, p) m. (j, p) n. (e, k) o. (e, q) p. (k, q)

A5. For the conditions in Fig. 22.2, find the angle of refraction in <u>water</u>, given an incident angle of 45° in air for λ (μm) of

a. 0.4 b. 0.45 c. 0.5 d. 0.55e. 0.6
f. 0.65 g. 0.7 h. 0.42 i. 0.47 j. 0.52
k. 0.57 m. 0.62 n. 0.67

A6. For green light, calculate the angle of refraction for: (i) water, and (ii) ice, given the following incident angles in air, for conditions in Fig. 22.2:

a. 5° b. 10° c. 15° d. 20° e. 25° f. 30° g. 35°
h. 40° i. 45° j. 50° k. 55° m. 60° n. 65° o. 70°
p. 75° q. 80° r. 85°

A7. For Snell's law in 3-D, given the following component angles in degrees (α_1, β_1), find the total incident angle (θ_1) in degrees.

a. 5, 20 b. 5, 35 c. 5, 50 d. 5, 65 e. 5, 80
f. 20, 35 g. 20, 50 h. 20, 65 i. 20, 80 j. 35, 50
k. 35, 65 m. 35, 80 n. 50, 65 o. 50, 80 p. 65, 80

A8. Using the incident components in air from the previous problem, find the refraction components of blue-green light in ice. Check your answers using Snell's law for the total refraction angle. Assume the refractive index in air is 1.0 and in ice is 1.31 .

A9. Use the data in Fig. 22.2 to calculate the critical angles for light moving from ice to air, for λ (μm) of

a. 0.4 b. 0.45 c. 0.5 d. 0.55e. 0.6
f. 0.65 g. 0.7 h. 0.42 i. 0.47 j. 0.52
k. 0.57 m. 0.62 n. 0.67

A10. Same as the previous exercise, but for light moving from water to air.

A11. Find the reflectivity from spherical raindrops, given impact parameters of:
a. 0.0 b. 0.1 c. 0.2 d. 0.3 e. 0.4 f. 0.5
g. 0.6 h. 0.7 i. 0.75 j. 0.8 k. 0.85 m. 0.9
n. 0.95 o. 0.98

A12. What value(s) of the impact parameter gives a primary-rainbow viewing angle of $\theta_1 = 42.0°$ for light of the following wavelength (μm)?
a. 0.4 b. 0.45 c. 0.5 d. 0.55e. 0.6
f. 0.65 g. 0.7 h. 0.42 i. 0.47 j. 0.52
k. 0.57 m. 0.62 n. 0.67

A13. Find the output viewing angle for a primary rainbow with the conditions in Fig. 22.2 for green light and the following impact parameters.
a. 0.5 b. 0.55 c. 0.6 d. 0.65 e. 0.7 f. 0.75
g. 0.8 h. 0.85 i. 0.9 j. 0.95

A14.(§) Use a spreadsheet to calculate and plot primary-rainbow viewing angles for a full range of impact parameters from 0 to 1, for the conditions in Fig. 22.2. Do this for light of wavelength (μm):
a. 0.4 b. 0.45 c. 0.5 d. 0.55e. 0.6
f. 0.65 g. 0.7 h. 0.42 i. 0.47 j. 0.52
k. 0.57 m. 0.62 n. 0.67

A15.(§) Same as previous exercise but for a secondary rainbow.

A16. For yellow light in a 22° halo, what is the viewing angle for the following input angles? Use the conditions in Fig. 22.2.
a. 15° b. 20° c. 25° d. 30° e. 35°
f. 40° g. 45° h. 50° i. 55° j. 60°
k. 65° m. 70° n. 75° o. 80° p. 85°

A17. Same as the previous exercise, but for blue light.

A18.(§) Use a spreadsheet to generate curves for green light, similar to those drawn in Fig. 22.25 for the 22° halo. Use the conditions in Fig. 22.2.

A19.(§) Same as previous exercise, but for the 46° halo.

A20. For yellow light in a 46° halo, find the viewing angle for the following input angles. Use the conditions in Fig. 22.2.
a. 58° b. 60° c. 62° d. 64° e. 66° f. 68° g. 70°
h. 72° i. 74° j. 76° k. 78° m. 80° n. 82°
o. 84° p. 86° q. 88°

A21. Same as the previous exercise, but for blue light.

A22. Find the minimum viewing angle (i.e., the nominal halo angle) for green light using the conditions in Fig. 22.2 for the following ice-crystal wedge angle:
a. 25° b. 52.4° c. 56° d. 60° e. 62° f. 63.8°
g. 70.5° h. 80.2° i. 90° j. 120° k. 150°

A23. For a solar elevation of 10° and conditions as in Fig. 22.2, calculate the viewing angle components for a circumzenithal arc for red light with a crystal rotation of $\beta =$
a. 10° b. 12° c. 14° d. 16° e. 18° f. 20°
g. 22° h. 24° i. 26° j. 28° k. 30°
m. 32° n. 34°

A24.(§) For conditions as in Fig. 22.2, calculate and plot circumzenithal arcs similar to Fig. 22.33 for red and violet light, but for solar elevation angles of
a. 10° b. 12° c. 14° d. 16° e. 18° f. 20°
g. 22° h. 24° i. 26° j. 28° k. 30° m. 0°
n. 2° o. 4° p. 6° q. 8°

A25. For a solar elevation of 10°, calculate the viewing angle components for a sun dog for red light with the following crystal rotations β. Use the conditions in Fig. 22.2.
a. 15° b. 20° c. 25° d. 30° e. 35°
f. 40° g. 45° h. 50° i. 55° j. 60°
k. 65° m. 70° n. 75° o. 80° p. 85°

A26.(§) Calculate and plot sun dog arcs similar to Fig. 22.35, but for the following solar elevation angles. Use the conditions of Fig. 22.2 for green light.
a. 5° b. 15° c. 25° d. 30°
e. 35° f. 45° g. 50° h. 55° i. 60°

A27.(§) For $\gamma = 80°$, plot upper tangent arc elevation and azimuth angles for a ray of orange-yellow light, for a variety of evenly-space values of rotation angle. Use a solar elevation of:
a. 10° b. 12° c. 14° d. 16° e. 18° f. 8°
g. 22° h. 24° i. 26° j. 28° k. 30°
m. 32° n. 34° o. 36° p. 38° q. 40°

A28. Find the fraction of incident light that is scattered for an optical thickness of:
a. 0.01 b. 0.02 c. 0.05 d. 0.10 e. 0.2
f. 0.5 g. 1. h. 2 i. 3 j. 4
k. 5 m. 7 n. 10 o. 20 p. 50

A29. What fraction of incident red light is scattered from air molecules along a horizontal path near the Earth's surface, with path length (km) of

a. 0.5 b. 1 c. 2 d. 5 e. 10 f. 20 g. 50
h. 100 i. 200 j. 500 k. 1000 m. 2000

A30.(§) Calculate and plot the relative fraction of scattering as a function of wavelength, for Rayleigh scattering in air.

A31. For cloud droplets of 5 μm radius, find the corona fringe viewing angles for the 2nd through 8th fringes, for light of the following wavelength (μm):
a. 0.4 b. 0.45 c. 0.5 d. 0.55e. 0.6
f. 0.65 g. 0.7 h. 0.42 i. 0.47 j. 0.52
k. 0.57 m. 0.62 n. 0.67

A32.(§) Calculate and plot the viewing angle vs. wavelength for the:
a. second corona fringe.
b. third corona fringe.
c. fourth corona fringe.

A33. (§) Calculate and plot the ratio of refractive index in air to a reference refractive index in air, for a variety of values of ratio of air density to reference air density.

A34. If the temperature decreases 10°C over the following altitude, find the mirage radius of curvature of a light ray. Assume a standard atmosphere at sea level.
a. 1 mm b. 2 mm c. 3 mm d. 4 mm
e. 5 mm f. 6 mm g. 7 mm h. 8 mm
i. 9 mm j. 1 cm k. 2 cm m. 3 cm
n. 4 cm o. 5 cm p. 10 cm q. 20 cm

22.8.3. Evaluate & Analyze

E1. If light is coming from the water towards the air in Fig. 22.1 (i.e., coming along the θ_2 path but in the opposite direction), then sketch any incident and reflected rays that might occur.

E2. Salt water is more dense than fresh water. Sketch how light wave fronts behave as they approach the salt-water interface from the fresh water side.

E3. Is it possible for a material to have a refractive index less than 1.0 ? Explain.

E4. In general, how does the refractive index vary with temperature, pressure, and density?

E5. Use geometry and trig to derive eq. (22.6).

E6. Consider Fig. 22.5. If you were in a boat near the words "no escape here" and were looking into the water towards an object in the water at the black dot near the bottom of that figure, what would you see?

E7. Speculate on why rainbows are common with rain from cumulonimbus clouds (thunderstorms) but not with rain from nimbostratus clouds.

E8. If you were standing on a mountain top in a rain shower, and the sun was so low in the sky that sun rays were shining at a small angle upward past your position, could there be a rainbow? If so, where would it be, and how would it look?

E9. Use the relationship for reflection of light from water to describe the variations of brightness of a wavy sea surface during a sunny day.

E10. How does the intensity and color of light entering the raindrop affect the brightness of colors you see in the rainbow?

E11. Draw a sketch of a sun ray shining through a raindrop to make a primary rainbow. If red light is bent less than violet as a sun ray refracts and reflects through a raindrop, why isn't red on the inside of the primary rainbow instead of the outside?

E12. Use geometry to derive eq. (22.13).

E13. Use geometry to derive eq. (22.14).

E14. Draw a sketch of a sun ray path through a raindrop for a:
a. Tertiary rainbow b. Quaternary rainbow.
Your sketch must be consistent with the viewing angle listed for these rainbows.

E15. During the one reflection or two reflections of light inside a raindrop for primary and secondary rainbows, what happens to the portion of light that is not reflected? Who would be able to see it, and where must they look for it?

E16. Why are higher-order rainbows fainter than lower-order ones?

E17. If neither the primary or secondary rainbows return light within Alexander's dark band, why is it not totally black?

E18. Compare and contrast a twinned rainbow and supernumerary bows.

E19. Often hexagonal column ice crystals in the real atmosphere have indentations in their basal faces. These are known as hollow columns. How might that affect ice-crystal optical phenomena?

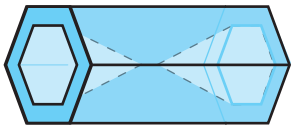

E20. For hexagonal columns, what other crystal angles exist besides 60° and 90°? For these other crystal angles, at what viewing angles would you expect to see light from the crystal?

E21. In Fig. 22.18, why are plate-crystal wobble and column-crystal rotation necessary to explain a sun pillar?

E22. Fig. 22.18d shows a dendrite ice crystal. In addition to the sun pillar, for what other halos & optical phenomena might such dendrites be important?

E23. Fig. 22.22a has only reflection while Fig. 22.22b also has two refractions. How might this affect the color of subsuns?

E24. Eq. (22.15) does not consider the finite size of a hexagonal column. What range of input angles would actually allow rays to exit from the face sketched in Fig. 22.24 for 22° halos?

E25. Use geometry to derive eq. (22.15) for the 22° halo.

E26. Derive equation (22.16) for the minimum viewing angle for halos. (You might need calculus for this).

E27.(§) Suppose a halo of 40° was discovered. What wedge angle β_c for ice would cause this?

E28. When the sun is on the horizon, what is the angle between the 22° halo and the bottom of the circumzenithal arc?

E29. Is it possible to see both a circumzenithal and a circumhorizonal arc at the same time? Explain.

E30 Why might only one of the sun dogs appear?

E31. Using geometry, derive the minimum thickness to diameter ratio of hexagonal plates that can create sun dogs, as a function of solar elevation angle.

E32. For both sun dogs and rainbows, the red color comes via a path from the sun to your eyes that does not allow other colors to be superimposed. However, for both phenomena, as the wavelength gets shorter, wider and wider ranges of colors are superimposed at any viewing angle. Why, then, do rainbows have bright, distinct colors from red through violet, but sundogs show only the reds through yellows, while the large viewing angles yield white color rather than blue or violet?

E33. Why are the tangent arcs always tangent to the 22° halo?

E34. Sometimes it is possible to see multiple phenomena in the sky. List all of the optical phenomena associated only with

a. large hexagonal plates
b. large hexagonal columns
c. small hexagonal columns
d. small hexagonal plates
e. large hexagonal pyramids

E35. If optical depth is defined as the optical thickness measured vertically from the top of the atmosphere, then sketch a graph of how optical depth might vary with height above ground for a standard atmosphere.

E36. If you take photographs using a polarizing filter on your camera, what is the angle between a line from the subject to your camera, and a line from the subject to his/her shadow, which would be in the proper direction to see the sky at nearly maximum polarization? By determining this angle now, you can use it quickly when you align and frame subjects for your photographs.

E37 In the Solar & Infrared Radiation chapter, Beer's law was introduced, which related incident to transmitted light. Assume that transmitted light is 1 minus scattered light.

a. Relate the Rayleigh scattering equation to Beer's law, to find the absorption coefficient associated with air molecules.

b. If **visibility** is defined as the distance traveled by light where the intensity has decreased to 2% of the incident intensity, then find the visibility for clean air molecules.

c. Explain the molecular scattering limit in the atmospheric transmittance curve of Fig. 8.4a in the Satellite & Radar chapter.

E38. Discuss the problems and limitations of using visibility measurements to estimate the concentration of aerosol pollutants in air.

E39. For atmosphere containing lots of 1.5 μm diameter sulfuric acid droplets, describe how the sky and

sun would look during a daily cycle from sunrise past noon to sunset.

E40. To see the brightest fringes furthest from the sun during a corona display, what size cloud droplets would be best?

E41. If you were flying above a cloud during daytime with no other clouds above you, describe why you might not be able to see glory for some clouds.

E42. Contrast and compare the refraction of light in mirages, and refraction of sound in thunder (see the Thunderstorm chapter). Discuss how the version of Snell's law in the Thunderstorm chapter can be applied to light in mirages.

E43. Microwaves are refracted by changes in atmospheric humidity. Use Snell's law or Huygens' principle to describe how ducting and trapping of microwaves might occur, and how it could affect weather radar and air-traffic control radar.

E44. What vertical temperature profile is needed to see the Fata Morgana mirage?

E45. Green, forested mountains in the distance sometimes seem purple or black to an observer. Also, the mountains sometimes seem to loom higher than they actually are. Discuss the different optical processes that explain these two phenomena.

E46. Paint on traffic signs and roadway lines is often sprinkled with tiny glass spheres before the paint dries, in order to make the signs more reflective to automobile headlights at night. Explain how this would work. Also, would it be possible to see other optical phenomena from these glass spheres, such as rainbows, halos, etc? Justify your answer.

22.8.4. Synthesize

S1. Suppose atmospheric density were (a) constant with height; or (b) increasing with height. How would optical phenomena be different, if at all?

S2. How would optical phenomena be different if ice crystals were octagonal instead of hexagonal?

S3. Suppose the speed of light through liquid and solid water was faster than through air. How would optical phenomena be different, if at all?

S4. After a nuclear war, if lots of fine Earth debris were thrown into the atmosphere, what optical phenomena would cockroaches (as the only remaining life form on Earth) be able to enjoy?

S5. Using the data in Fig. 22.2, fit separate curves to the refractive index variation with wavelength for air, water, and ice. Can you justify any or all of the resulting equations for these curves based on physical principles?

S6. Knowing the relationship between optical phenomena and the cloud (liquid or water) microphysics, and the relationship between clouds and atmospheric vertical structure, cyclones and fronts, create a table that tells what kind of weather would be expected after seeing various optical phenomena.

S7. If large raindrops were shaped like thick disks (short cylinders) falling with their cylinder axis vertical, how would rainbows be different, if at all?

S8. If large ice crystals were shaped like cylinders falling with their cylinder axis horizontal, how would ice-crystal optics be different, if at all?

S9. Consider Fig. 22.5. Could a thin layer of different fluid be floated on the liquid water to allow all light ray angles to escape from liquid to air? Justify your proposal.

S10. If there were two suns in the sky, each with light rays going to the same raindrop but arriving from different angles, is there a special angle between the arriving sun rays such that the two separate rainbows reinforce each other to make a single brighter rainbow?

S11. Design an ice-crystal shape that would cause:
a. different halos and arcs than exist naturally.
b. a larger number of natural halo and arcs to occur simultaneously.

S12. Suppose raindrops and ice crystals could cause refraction but not reflection or diffraction. What atmospheric optical phenomena could still exist? Justify your answers.

S13. Suppose that spacecraft landing on other planets can photograph optical phenomena such as halos, arcs, bows, etc. Describe how you could analyze these photographs to determine the chemicals and/or temperature of these planetary atmospheres.

S14. Design equipment to be used in the Earth's atmosphere that could determine the vertical temperature profile by measuring the characteristics of mirages.